# SOIL CARBON STOCKS AND GREENHOUSE GAS FLUXES QUANTIFICATION IN SELECTED SMALLHOLDER FARMERS' LAND UTILIZATION TYPES OF SIAYA COUNTY, KENYA

**ESPHORN KIBET**

**A THESIS SUBMITTED IN PARTIAL FULFILMENT OF THE REQUIREMENT FOR THE AWARD OF THE DEGREE OF MASTER OF SCIENCE IN LAND AND WATER MANAGEMENT OF THE UNIVERSITY OF EMBU**

**SEPTEMBER 2022**

## DECLARATION

This thesis is my original work and has not been presented elsewhere for a degree or any other award.

Signature……………………………… Date ……………………

**Esphorn Kibet**

Department of Water and Agricultural Resource Management

A509/1353/2019

This thesis has been submitted for examination with our approval as University Supervisors.

Signature……………………………… Date ……………………

**Dr. Onesmus Ng'etich**

Department of Water and Agricultural Resource Management

University of Embu

Signature……………………………… Date ……………………

**Dr. Milka Kiboi**

Division of Research, Innovation, and Outreach

KCA University

Signature……………………………… Date ……………………

**Prof. Felix Ngetich**

Department of Plant, Animal and Food Sciences (PAFS),

Jaramogi Oginga Odinga University of Science and Technology (JOOUST)

# DEDICATION

I dedicate this thesis to the people who supported my studies. Thanks for making this journey a reality.

## ACKNOWLEDGEMENT

I wish to appreciate the Kenya Climate-Smart Agriculture Project (KCSAP), a world bank-funded multi-disciplinary collaborative project titled: "*Validating Sustainable Land Management Technologies for Enhanced Carbon Sequestration and Improved Smallholder Farmer's Livelihoods*" that I was able to benefit from as a field technician, courtesy of the below-ground carbon team. I would like to thank my supervisors, Dr. Onesmus Ngetich, Dr. Milka Kiboi, and Prof. Felix Ngetich, for their support and guidance throughout my studies. I am also thankful to my mentor, Collins Musafiri, who guided me in field experimentation and greenhouse gas analysis throughout my studies. I acknowledge Mazingira laboratories for the analysis of greenhouse.

Also, I would like to thank the farmer for providing a farm for my research work, Levi Ngetich for always pushing me and providing mentorship and my family members for their encouragement and moral support.

## TABLE OF CONTENTS

**CONTENTS**

## LIST OF TABLES

## LIST OF FIGURES

## LIST OF ABBREVIATIONS AND ACRONYMS

| | |
|---|---|
| AEZ | Agro Ecological zone |
| ANOVA | Analysis of Variance |
| BD | Bulk Density |
| CCD | Climate Change Directorate |
| CIDP | County Integrated Development Plan |
| DAP | Diammonium Phosphate |
| DNDC | DeNitrification-DeComposition |
| DOC | Dissolved Organic Carbon |
| ECD | Electron Capture Detector |
| FID | Flame Ionization Detector |
| GC | Gas Chromatography |
| GHG | Greenhouse Gas |
| HSD | Honestly Significance Difference |
| IPCC | Intergovernmental Panel on Climate Change |
| LM | Lower Midland |
| LUT | Land Utilization Type |
| ME | Mean Error |
| NDCs | Nationally Determined Contributions |
| NRMSE | Normalized Root Mean Square Error |
| NSE | Nash-Sutcliffe Efficiency |
| OM | Organic Matter |
| RMSE | Root Mean Square Error |
| SOC | Soil Organic Carbon |
| SSA | Sub-Saharan Africa |
| UNFCCC | United Nations Framework Convention on Climate Change |

## GENERAL ABSTRACT

The up-surging population in sub-Saharan Africa (SSA) has led to the conversion of forests to agricultural land leading to greenhouse gas (GHG) emissions. The resilient land utilization types are key in soil carbon sequestration. There is a vast data gap for the National and regional greenhouse gas (GHG) budget from different smallholders' land utilization types in Kenya and sub-Saharan Africa (SSA). This study aimed to quantify carbon stock and greenhouse gas fluxes from different land utilization types (LUT) in Siaya. The LUTs considered in the study were agroforestry M (agroforestry with *Markhamia lutea*), sole sorghum, agroforestry L (agroforestry with *Leucaena leucocephalaI*), sole maize, and grazing land replicated thrice. Soil samples were collected at a depth of 0-5, 5-10, 10-20, and 20-30cm from different LUTs to determine soil bulk density, organic carbon (SOC) concentration, and carbon stock. PROC ANOVA was used to determine the significant difference in soil bulk density, SOC %, SOC stock. Additionally, GHG data were subjected to analysis of variance (ANOVA) using SAS 9.4 software. Before analysis, the normality of soil GHG fluxes was tested using the Shapiro-Wilk test. DeNitrification-DeComposition (DNDC) model was also used to simulate GHG gases. Soil bulk density varied significantly ($p$<0.05) across the LUTs and soil depths with a range of 1.30 and 1.60gcm$^{-3}$ under Agrofestry M and grazing land, respectively, at 0-5cm depth. A significant difference ($p$<0.0001) in SOC concentration was observed with high SOC concentration under Agroforestry M of 30.14gCkg$^{-1}$ at 0-5cm depth than all the other treatments and low SOC (8.4g Ckg$^{-1}$) in sole maize. Soil organic carbon stocks significantly ($p$<0.0001) varied across LUTs and depths. There was high carbon stock in agroforestry M (19622 kg C ha$^{-1}$) and grazing land (20069.7kgCha$^{-1}$) at 0-5 cm. Soil GHG fluxes significantly varied across the LUTs methane $p$<0.05, Carbon diode $p$=0.05, and nitrous oxide $p$=0.05. The cumulative methane fluxes ranged from -0.35 kg $CH_4$-C ha$^{-1}$ in grazing land highest -1.05 kg $CH_4$-C ha$^{-1}$ sole maize. Low soil $CO_2$ emissions under sole maize, 6510 kg $CO_2$-C ha$^{-1}$, and the highest under grazing land were observed, 14401 kg $CO_2$-C ha$^{-1}$. The results showed the lowest soil $N_2O$ fluxes under grazing land, 0.69 kg $N_2O$-Nha$^{-1}$, and the highest under agroforestry L 2.48 kg $N_2O$-N ha$^{-1}$. The model showed a high degree of fit in simulating daily soil temperature, soil moisture, and soil $N_2O$ emissions. The model depicted good results during simulation of soil moisture; root mean square error (RMSE) <5, 2% < normalized root means square error (nRMSE) <15.54%, 0.86< modelling efficiency (NSE) (NSE) <0.99, 0.03< coefficient of determination (R$^{2)}$ <0.97 and (index of agreement) d < 0.99. Daily soil temperature; 0.08 <RMSE< 1.33, from 0.3%< nRMSE< 5.9%, from 0.27< NSE< 0.99, from 0.12< $R^2$ <0.99. daily soil $N_2O$; 0.002 <RMSE< 0.006, 0.45% <nRMSE< 2.48%, NSE=0.99, from 0.5< $R^2$ <0.9, 0.98 <d< 0.99. The DNDC model showed relatively good results in simulating soil moisture, temperature, and $N_2O$ fluxes. The model showed relatively fitted $N_2O$ emissions peaks following the precipitations across all the LUTs. The model had good to excellent performance in simulating the $N_2O$ fluxes. The drivers of soil GHG were soil bulk density, soil organic carbon, soil moisture, clay content, and root production during GHG simulation and estimation. The results thus help fill the gaps in the national and regional data on carbon and emissions budgets.

# CHAPTER ONE

# GENERAL INTRODUCTION

## 1.1 Background information

Smallholder farmers subject their land utilization types to changes to meet the surging population's demand and cope with climate change. The process could have an adverse effect on soil organic carbon stocks. Different land utilization types have varying potentials to store carbon, with agroforestry gaining global interest due to its ability to store huge carbon stocks (Kim et al., 2016) compared to croplands. Similarly, grazing could have a serious influence on soil organic carbon due to vegetation disturbance (Kumi et al., 2021), hence altering the carbon input-output balance (Namirembe et al., 2020). Varying vegetation and the type of management practices, such as; tillage, could significantly influence carbon (Kiboi et al., 2020). Cultivation raises carbon loss by increasing soil microbial activities (Swanepoel et al., 2016). Further, changes in land utilization types can significantly impact the soil organic carbon stock with the tendency to decrease soil organic carbon with an increase in productivity (Williams et al., 2018). In addition, change in cropping systems (Henry et al., 2009) contributes to the variability of soil organic carbon stock attributed to a different rate of photosynthesis by different plants hence balancing the ecosystems by reducing the amount of greenhouse (GHG) fluxes. There is a paucity of data inventories on SOC due to its dynamics attributed to changes in land utilization types.

The change in land utilization can either increase carbon inputs or lead to a decrease in carbon inputs. About 78% of carbon is stored in soil compartments (Huang et al., 2012) which can be altered through anthropogenic activities such as tillage and grazing. To counteract the reduction of carbon across the land utilization types, farmers should honor the 4 per a thousand initiative (http://4p1000.org/), a worldwide healthy and carbon rich soils to combat climate and improve on food security. However, the conversion of more land for crop production with low soil amendment goes against the aim of the 4/1000 initiative. Agriculture could be a remedy to climate change by improving ways of farming and practicing sustainable farming that aims at reducing greenhouse gas (GHG) production (Smith et al., 2016). Reducing GHG emissions is adversely influenced by reduced land holdings in the study area (County Integrated Development Plan (CIDP).

Siaya County. 2018;2022).

Land utilization plays a fundamental role in GHG production due to varied SOC and N concentrations in soil compartments. Land management practices, including crop residue retention, greatly impacts the SOC (Bolinder et al., 2020) and, consequently, GHG emissions. The application of fertilizers and manure from livestock could double GHG emissions (Hickman et a., 2011). The GHGs (carbon dioxide $CO_2$, methane $CH_4$, and nitrous oxide $N_2O$) are products of different biogeochemical processes (Butterbach- Bahl et al., 2013). The heterotrophic respiration yields $CO_2$ (Ren et al., 2022), methanogenesis yields $CH_4$ (Kennedy-Perkins, 2022), while nitrification and denitrification yield $N_2O$ (Butterbach- Bahl et al., 2013). Therefore, agricultural activities that alter soil climate leads to the production of trace gas emissions. Additionally, anthropogenic factors also contribute to GHG emissions. The process hinders understanding GHG fluxes (Hickman et al., 2014). Hence, the need to quantify soil trace gas emissions across different land utilization types.

United Nations Framework Convention on Climate Change (UNFCC) conference of 2015 in Paris launched an initiative to increase agroecosystem carbon sequestration and reduce GHG fluxes by improving agricultural management activities (The Paris agreement). Being a signatory of the Paris Agreement 2015, Kenya is obligated to report their National Determined Contributions (NDC) of GHG fluxes. The Kenyan government has established Climate Change Directorate (CCD) to coordinate low carbon and climate-resilient pathways to reduce GHG fluxes by 30 % by 2030 (Radeny et al., 2020). The previous Kenya NDCs report documented agriculture (40%) as the primary source of GHG fluxes nationally (Radeny et al., 2020). Hence the need for accurate quantification of soil GHG fluxes across different agricultural sectors, including smallholders' land-utilization types. Accurate GHG fluxes data across different smallholder land-utilization types is fundamental to improving Kenyans' reporting of NDCs to the UNFCCC.

Despite the need by the Paris agreement signatories to report their NDC, GHG in-situ measurements are essentially expensive (Giltrap et al., 2010). Therefore, using biogeochemical models is novel in evaluating and quantifying soil GHG fluxes. Models provide quick soil GHG assessment. One of the widely used biogeochemical models is the DeNitrification DeComposition (DNDC) model, which has been used in agro-ecosystems to simulate trace gas emissions (Li et al., 1992a; Li et al., 1994). The DNDC model has been used in Kenya to simulate soil GHG fluxes and maize performance under different soil fertility management technologies (Macharia et al., 2021; Musafiri et al., 2021). Using the DNDC model offers an opportunity for understanding C and N dynamics and provides opportunities for GHGs emissions mitigation. There is still limited information on the applicability of the DNDC model in simulating agricultural trace gas emissions from different land utilization types.

## 1.2 Statement of the problem

Smallholder farmers change their land utilization types to increase climate change resilience and improve their livelihood. The diversification may significantly influence SOC stock and greenhouse gas budget in Siaya County and Kenya at large. Kenya is obligated to report her Nationally Determined Contributions of greenhouse gases to the UNFCCC. Despite the need for accurate soil GHG fluxes data, only a few studies have been conducted to quantify soil GHG fluxes in Kenya across different smallholders' land utilization types; thus, a dearth of directly quantified GHG fluxes data. Additionally, there is scanty information on the contribution of whole-farm smallholders' land-utilization types on soil carbon stock and GHG fluxes in Siaya County. Direct quantification of soil GHG fluxes to inform NDCs is complex, time-consuming, and expensive. This calls for robust methodologies, including modeling to validate GHG emissions across different smallholders' land-utilization types.

## 1.3 Justification of the Study

The SOC variability and depletion lead to soil fertility and agricultural production changes. The upsurging population coupled with climate change has increased the need for smallholder farmers to subject their land to different utilization types. This raises the uncertainty on the SOC across the land utilization types attributed to different land management systems. The change of SOC could lead to an acceleration in GHG emissions hence climate change. Quantification of SOC, therefore, enables sustainable land utilization and climate mitigation. The uncertainty of GHG emissions is still unclear due to land utilization change and the uniqueness of land utilization types. To honor the Paris Agreement, Kenya is obligated to report her NDC to UNFCCC for climate mitigation.

This study, therefore, aids in improving Kenya's accuracy in reporting her NDC by quantifying GHG fluxes across smallholders' land utilization types and simulating GHG fluxes by using DNDC and inform policy formulations by both county and national government.

## 1.4 Research Objectives

### 1.4.1 General objective

The general objective was to quantify soil carbon stocks and GHG fluxes in selected smallholders' land utilization types in Siaya County, Kenya.

### 1.4.2 specific objectives:

1. To quantify soil carbon stocks of selected land utilization types in smallholder farms in Siaya County.
2. To quantify agricultural greenhouse gas emissions of selected land utilization types of smallholder farms in Siaya County.
3. To validate greenhouse gas emissions of selected land utilization types in smallholder farms using DNDC model in Siaya County.

## 1.5 Research questions

1. How does soil carbon stock differ across selected land utilization systems in Siaya County?
2. How does soil GHG emissions vary across the selected land utilization system in Siaya County?
3. How well does the DeNitrifiaction-DeComposition model simulate soil GHG fluxes in selected land utilization systems in Siaya County?

## 1.6 Thesis outline

This thesis comprises five chapters. Chapter one has the introductory section with background information on the study, a statement of the problem, the justification, and the research objectives. Chapter two to four presents the individual objective studies in paper format. Chapter five details the thesis synthesis, conclusions, recommendations, and areas for further research.

Chapter two presents the SOC stock quantification under different land utilization types.

The soil samples were collected for analysis of SOC across the five land utilization types of Siaya County. The effects of LUTs on soil bulk density and soil texture are also presented. Chapter three presents the effects of LUTs on the soil GHG fluxes. The chapter illustrates soil properties affecting GHG fluxes such as; SOC, soil bulk density, carbon fractions, and yield-scale emissions. Chapter four presents soil GHG simulation under different LUTs in the study area. Soil moisture and soil temperature simulation are also presented in this chapter. It also presents the DNDC input parameters that were used during GHG simulation.

# CHAPTER TWO

## SOIL ORGANIC CARBON STOCKS UNDER DIFFERENT LAND UTILIZATION TYPES OF SIAYA COUNTY, KENYA


### Abstract

The up-surging population in sub-Saharan Africa (SSA) has led land being open up for agricultural purposes. The resilient land utilization types that are key in carbon sequestration as per "4 per a mile" initiative are not fully realized. Hence, limited data on different land utilization types' contribution to climate change mitigation through carbon input to soils. To quantify carbon stock across different land utilization types (LUT) practiced in Siaya County; 1) Agroforestry M (Agroforestry *Markhamia lutea* and sorghum*)*, 2) sole sorghum (sorghum monocrop), 3) Agroforestry L (*Leucaena leucocephala)*, 4) sole maize (maize monocrop), and 5) grazing land were studied. Soil organic carbon (SOC) concentration, soil carbon stock, and soil bulk density in the selected land utilization types were determined. The treatments were replicated thrice at depths of 0-5, 5-10, 10-20, and 20-30cm. Soil bulk density varied significantly ($p$<0.0001) at 0-5 cm across the LUTs. There was low at 20-30cm under grazing land. Conversely, the soil bulk density was high at 0-5cm under grazing land (1.6 g $cm^{-3}$). Low SOC (8.4g C $kg^{-1}$) in sole maize and high SOC concentration was observed under Agroforestry M of 30.14gC$kg^{-1}$ at 0-5cm than all the other treatments. There was a significant ($p$<0.0001) difference in SOC stock across the LUTs and depths. There was high carbon stock in agroforestry M (19622 kg C $ha^{-1}$) and grazing land (20069.7kgC$ha^{-1}$) at 0-5 cm. In agroforestry L, a high carbon was observed at 10-20 and 20-30 cm (26913 and 26913.1kgC$ha^{-1}$, respectively). Overall, the different LUTs showed varied SOC accumulation at different depths. The findings highlight that agroforestry L and agroforestry M are promising interventions toward climate mitigation through carbon induction to soils.



**Keywords**: Land utilization type, soil carbon stocks, Siaya county, agroforestry

## 2.1 Introduction

Land use alters ecosystems' function and structure of the ecosystem, which can either increase or decrease carbon stock and consequently affect biodiversity (Guo et al., 2020). Generally, about 78.6% of carbon is stored in soil compartments (Huang et al., 2012). Carbon plays a fundamental role in agronomic production, soil fertility, and ecosystem health (Gonçalves et al., 2017; Smith et al., 2016). However, with the increase in population, more land has been degraded due to limited available land (Kanyenji et al., 2020), thus, lowering crop production (Vanlauwe et al., 2017). To increase carbon input to soil and reduce the incidence of climate change, farming systems and land utilization should honor the 4/1000 initiative (http://4p1000.org/) accessed on 4 April 2022, that aims to increase the amount of carbon by 4% to 40 cm in depth. Ideally, the initiative aims at improving on sustainability and ending hunger through increasing carbon in soils. The change of more land for crop production has significantly led to decreased carbon concentration and stocks and, consequently, increased anthropogenic greenhouse gas emissions. Agriculture contributes 14-17% of global greenhouse gas emissions (GHG) through changes in land utilization and intensification of agricultural activities (Valentin et al., 2014). Agriculture is sought to remedy climate change by implementing sustainable farming practices that increase carbon input in soils (Smith et al., 2016; Somer et al., 2017). This can reduce GHG emissions by 5-15% (Smith et al., 2008a). In Kenya, the increasing population has led to the conversion of more land to croplands to meet the dietary needs to curb food insecurity (Vanlauwe et al., 2017). The diversity of land utilization has been necessitated by reduced land holding, especially in Western Kenya (Henry et al., 2009). The change in land utilization types may significantly influence soil organic carbon (SOC) in soil compartments.

Diverse land utilization types include; grazing lands (intensively controlled grasslands, pasture lands), agroforestry systems (afforestation and general agroforestry systems, home gardens), and intensively managed croplands (the annual and perennial crops) (Henry et al., 2009; Abegaz et al., 2020; Wachiye et al., 2020). Among these, the grazing land contribution to carbon alteration is under dispute as researchers have come up with mixed findings. While Qiu et al. (2013), Reszkowska et al. (2011), and Zuo et al. (2008) found a reduction in carbon stock under intense grazing, Silveira et al. (2014); Wei et al. (2011) found increasing carbon storage under grazing. Poor farming technologies in

Kenya have significantly affected soil health and food production (Vanlauwe et al., 2015). The situation has been adversely affected carbon dynamics in the region (Sommer et al., 2018), thus modifying biological diversity. The situation in the Western region is aggravated by high land subdivision coupled with low farm holdings (Henry et al., 2009; Siaya County Integrated Development Plan, 2018). The introduction of agroforestry systems has led to increased agricultural productivity attributed to massive carbon inputs. According to a review by Kim et al. (2016), agroforestry systems proved advantageous in crop production and increasing soil restoration, especially with leguminous trees (Brakas and Aune, 2011; Cardinael et al.,2015). Adopting agroforestry improved carbon inputs to soil compartments and reduced greenhouse gas emissions (Smith et al., 2016). Cultivation and cropping intensity reduce carbon in soils (Luo et al.,2010; Francaviglia et al., 2012). On the other hand, croplands are thought to lower carbon inputs in the study area (Kanyenji et al., 2020).

The SOC stock is a predictor of soil quality and health, used as a measurable component of soil organic matter (SOM) (Degu et al., 2019). Soil organic carbon is driven by; site characteristics, environment (Gonçalves et al., 2017), plant species (Sarto et al., 2020), and management practices (Nyawira et al.,2021; Ndung'u et al., 2021). Plants species play a vital role in SOC accumulation. The deep-rooted and high-density rooted plants have high SOC due to roots exudation and exfoliation. Further, water holding capacity, soil pH, and soil nutrients such as nitrogen and phosphorus concentration affect soil SOC (Guo et al., 2020). Soil's physical characteristics play a crucial role in regulating the rate of carbon input-output. Clay content protects organic carbon against microbial oxidation and helps carbon stabilization (Saidy et al., 2013). Conversely, an increase in sand content can lead to low soil SOC storage. Soil carbon stock can significantly affect soil bulk density (Morisada et al., 2004). However, Chaudhari et al. (2013) found a negative correlation between soil bulk density and SOC. Soil depth affects the SOC stock. Generally, SOC stock decreases with increasing depths' (Rahman et al., 2020; Guo et al., 2020; Kumi et al., 2021). Therefore, the variability of land utilization types could affect carbon due to varied soil characteristics.

Despite assorted works on carbon dynamics under croplands (Sommer et al., 2017; Kanyenji et al., 2020), knowledge of the effect of specific LUTs on SOC stock under the smallholder rainfed-dependent tropical farming systems is limited (Reppin et al., 2020). Thus, the study fills a data gap on the effects of LUTs on SOC stocks in smallholder farms. This study aims to evaluate the effects of LUTs on SOC stock across the soil profile (0–30 cm). The hypotheses backing this study are: (i) LUTs can vary soil organic carbon stock across soil profiles and (ii) soil bulk density can control SOC stock storage.

## 2.2 Materials and Methods

### 2.2.1 Study area

The study was conducted in smallholder farms (0˚01047.2700 S, 34˚16041.500 E) of the Nyajuok sub-location, Alego-Usonga sub-county, Siaya County, Kenya. The selected farms lie at approximately 1236 m above sea level. Nyajuok lies in the lower midland (LM1) agroecological zone (Jaetzold et al., 2010), mainly a sugarcane belt. The area experiences bimodal rainfall distribution with long rains (LR) season from March to July and short rains (SR) from August to December. The area receives long-term annual rainfall ranging between 1500 and 1900 mm and temperatures ranging from 20.9 to 21.8 °C. The SR season rainfall ranges between 600 and 800 mm, while an LR season ranges from 750 to 950 mm (Jaetzold et al., 2010). The soil type in the area is Ferralsols (Jaetzold et al., 2010), with declining soil fertility attributed to continuous cropping practices without amendments (De Groote et al., 2010). The main economic activity in the area is rain-fed agriculture, with a low farm holding per household of 1.0 ha (Siaya County Integrated Development Plan, 2018). The primary land utilization types include livestock grazing, agroforestry, and cereals (monocropping, intercropping). The smallholder farmers often intercrop cereals such as maize (*Zea mays*) and sorghum (*Sorghum bicolar)* with common beans (*Phaseolus vulgaris*), cowpeas (*Vigna unguiculata*), and soya beans (*Glycine max*) (Jaetzold et al., 2010).

### 2.2.2 Experimental design

The study design was farmer-designed and -managed (Type III). The smallholder farms were selected based on gradient homogeneity, soil type, and elevation. The study was conducted during the short rains of 2020 (SR 20) and the long rains of 2021 (LR 21). Five land utilization types under a similar soil type—Ferralsols—were selected; the homogeneity in farm characteristics aided in limiting errors and uncertainties of data quality. The selected land utilization types included (i) agroforestry with Markhamia lutea, (ii) sole sorghum, (iii) agroforestry with Leucaena leucocephala, (iv) sole maize, and (v) grazing land. In each land utilization type, measurements were conducted from three randomly established plots, with three replications.

### 2.2.3 Soil sampling

The undisturbed soil organic carbon and soil bulk density samples from four depths (0-5, 5-10, 10-20, and 20-30 cm) per land utilization type were collected using a 100cm$^3$ core ring (Eijkelkamp Agrisearch Equipment, Giesbeek, The Netherlands). The soil samples were collected in June 2021. Four soil samples from every land utilization type were taken, and the total number of samples resulted in 60. The soil texture samples were collected from 20 cm depth using a soil auger in each replicate of the selected land utilization type, then mixed by hand in a well labelled Zip Lock bag to form one composite sample totaling five samples. Samples were then transported to the laboratory for analysis.

### 2.2.4 Laboratory analysis

Soil texture was analysed following the hydrometer method and bulk density gravimetrically (Okalebo et al., 2002). Soil samples were passed through 2 mm sieve and analysed for soil organic carbon (SOC) following Walkely and Black wet oxidation method (Ryan et al., 2001). Percentage carbon (% C) was calculated using Equation 2.1.

$$CS = SOC \times Pb \times D \times 100 \qquad \text{Equation 2.1}$$

Where CS=carbon stock (kg C $ha^{-1}$), SOC=soil organic carbon concentration (g C $kg^{-1}$), Pb= soil bulk density (g $cm^{-3}$) and D=soil depth (cm)

### 2.2.5 Statistical analysis

Statistical analyses were performed using SAS 9.4 software. PROC ANOVA was used to determine the difference in soil bulk density, SOC %, and SOC stock between different LUTs and depths. Mean separation was done using Tukey's honestly significant difference (HSD) test at $p<0.05$. Simple Pearson correlation was used to determine the relationship between SOC and soil bulk density under LUTs and depths. Normality of data was done using Proc Univariate, where treatment, depths, and replicates were fixed factors while bulk density, SOC, and carbon stock were random factors.

## 2.3 Results and discussion

### 2.3.1 Soil texture

Table 2.1 shows soil characteristics of the five land utilization types. The soil had a high percentage of sand followed by silt in all the treatments. Sole maize had the highest percentage of sand (52%) and the lowest clay percentage (15%) was observed under sole sorghum. The soil texture was predominantly loam across the different land utilization types (Table 2.1).

**Table 2.1** Soil texture in different land utilization types of Alego-Usonga sub-county.

| LUT[1] | Sand (%) | Clay (%) | Silt (%) | Class |
|---|---|---|---|---|
| Agroforestry M | 47 | 18 | 34 | Loam |
| Sole sorghum | 48 | 15 | 37 | Loam |
| Agroforestry L | 46 | 18 | 36 | Loam |
| Sole Maize | 52 | 18 | 30 | Loam |
| Grazing land | 50 | 18 | 32 | Loam |

[1]LUT= land utilization types, Agroforestry M = Agroforestry with *Markhamia lutea*, sole sorghum, Agroforestry L= Agroforestry with *Leucaena leucocephala*, sole maize and grazing land.

Soil texture plays a fundamental role in soil nutrient management and the rate at which soil minerals translocate across the soil profile. The amount of clay content in soils predicts the rate of soil compaction (Degu et al., 2019), thus influencing the movement of SOC across the soil profile. However, in this study, the amount of silt and clay fractions across the land utilization type could not be linked to the amounts of carbon because of similar silt-clay concentrations. The results were consistent with findings by McLauchlan et al. (2006), who found no effects of clay concentration on carbon pools. However, Bruun et al. (2010) and Saidy et al. (2013) demonstrated that silt and clay fractions play a crucial role in stabilizing carbon. Additionally, clay fractions help in protecting carbon against microbial oxidation (Six et al., 2002). Gonçalves et al. (2017) reported a significant increase in microbial respiration and consequently loss of carbon from soil compartments with increasing silt and sand contents.

### 2.3.2 Soil bulk density in different land utilization types at different depths

There were significant ($p$<0.05) differences in soil bulk densities across the selected LUTs and soil depths (Figure 2.1). The soil bulk density in different LUTs and depths ranged from 1.24 to 1.61g $cm^{-3}$ (Figure 2.1). A significant ($p$<0.0001) difference was observed in soil bulk density at 0-5 cm depth across the LUTs; the variability ranged from 1.3 to 1.6 g $cm^{-3}$. The highest soil bulk density was under grazing land, while the lowest was in agroforestry M (Figure 2.1). There was a significant ($p$=0.02) difference at 5-10 cm depth with low distinction across LUTs. Nonetheless, sole sorghum had a high soil bulk density (1.44g$cm^{-3}$). There was also a significant (p=0.01) difference in bulk density at 10-20 cm and 20-30 cm depths, with grazing land having the lowest in both depths (Figure 2.1).

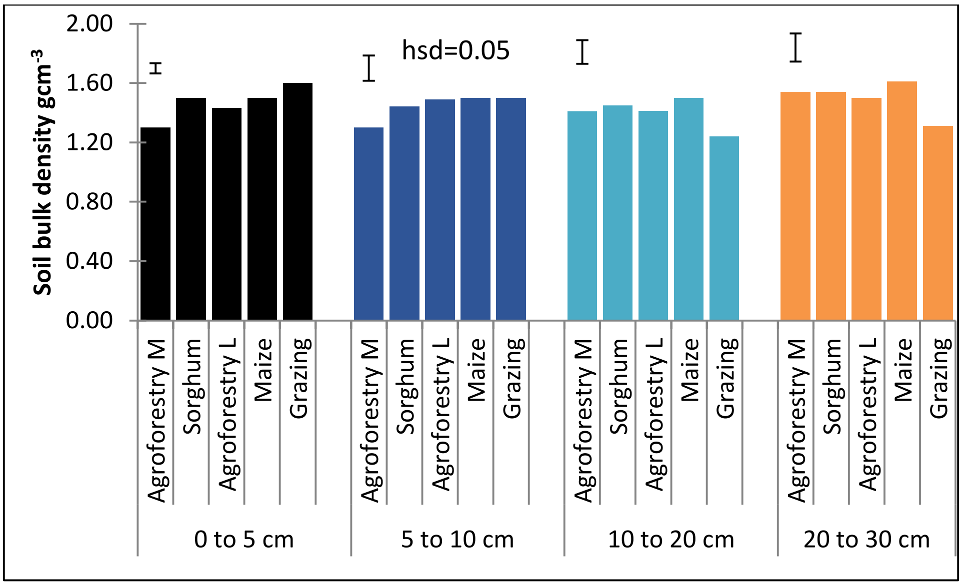


**Figure 2.1** Soil bulk density in different land utilization types (Agroforestry M = Agroforestry with *Markhamia luteai*; sole sorghum; Agroforestry L = Agroforestry with *Leucaena leucocephala*; sole maize; and grazing land) at different depths in Siaya County, Kenya ($p \leq 0.05$).

Soil bulk density is a fundamental soil parameter affected by soil clay content, soil aeration status, texture, general land utilization and the nutrient concentration in the soil (Tanveera et al., 2016). The soil bulk density findings corroborated with other studies done in SSA (Bikila et al., 2016; Sommer et al., 2018; Kiboi et al., 2020), that found soil bulk ranging from 1.2 to 1.5g$cm^{-3}$ under similar conditions. Results showed a high soil bulk density in sole sorghum, sole maize, and agroforestry L compared to the information obtained from the East African soil database (Hengl et al., 2017) of <1.3 g $cm^{-3}$. The results could have been attributed to low mechanical fracturing of soils that reduces soil bulk density (Degu et al., 2019).. Grazing land had high soil bulk density than all LUTs contrary to findings of Martin et al. (2016) found low soil bulk density under grazing land compared to cropland. Grazing land was the most compacted due to livestock trampling on upper depths, reducing microbial activities (Gao et al., 2019). Additionally, compaction in grazing land could have reduced macro-porosity, hence high BD on the upper depths (Anokye et al., 2021).

Agroforestry systems showed low bulk density that could be attributed to an increase in soil volume while reducing the soil mass due to high organic matter from leaf litterfall. Rahman et al. (2021) found low soil bulk density under oil palm cultivation. Further, Guo et al. (2020) found low soil bulk density under poplar plantations. Root penetrance might have increased the pore spaces in soil layers hence increasing air circulation, which necessitates the decomposition of organic matter in the soil layers by increasing microbial activities (Liao and Boutton, 2008; Vesterdal et al., 2002), thus low bulk density. The high bulk density at 0-5cm depths under the sole maize and sole sorghum could be attributed to soils' low organic matter (OM). Generally, the low soil amendments in sole maize and sole sorghum could have led to high soil bulk density (Islam and Weil, 2000).

### 2.3.3. Soil organic carbon contents in different land utilization types and depths

The variability of SOC contents in depths and LUTs ranged from 8.4 to 30.14 g C $kg^{-1}$. At the 0–5 cm depth, SOC differed significantly ($p < 0.0001$) among LUTs (Figure 2.2). The agroforestry M and grazing land had significantly high SOC contents than all LUTs (0–5 cm, Figure 2). A significant ($p = 0.0002$) difference in SOC contents was observed at the 5–10 cm depth. There was a higher SOC content in the agroforestry L and agroforestry M than in the sole maize and sole sorghum at the 5–10 cm depth (Figure 2.2). There was also a significant ($p < 0.0001$) difference in SOC concentration in the 10–20 cm and 20–30 cm depths, with high SOC contents of 19.15 and 18.06 g C $kg^{-1}$ under agroforestry L, respectively. In the sole maize, the SOC contents were low across all depths compared to all the LUTs. Decreasing SOC concentration with increasing soil depth was observed across the LUTs, except under agroforestry L (Figure 2.2).

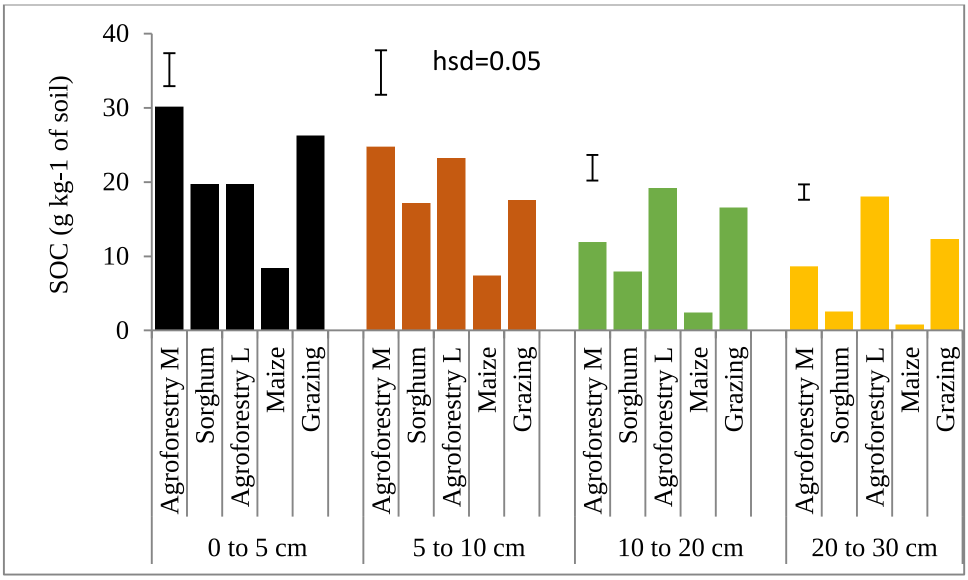


**Figure 2.2** Soil organic carbon (SOC) in different land utilization types (Agroforestry M= Agroforestry with *Markhamia luteai*, sole sorghum, Agroforestry L= Agroforestry with *Leucaena leucocephala*, sole maize and grazing land) at different depths in Siaya County, Kenya. a) SOC in % and b) SOC in g C $kg^{-1}$ of soil. ($p \leq 0.05$).

The decreasing SOC contents with increasing depths agrees with the study by Sommer et al. (2018), which showed a decrease in SOC with increasing depths. The results could be attributed to differences in Dissolve Organic Carbon (DOC) percolation attributed to varied soil bulk density and, consequently, the difference in micro-pores in the soil profile (Mishra et al., 2020). The variability of soil bulk density across LUTs contributed to the difference in SOC concentration. The study had varied soil bulk density at different depths and hence varied SOC, similar to findings of Kadiri et al. (2021). Generally, the decrease in SOC in-depth corroborates with the findings by Song et al. (2016) who found a decreasing SOC under similar conditions. The concentration of SOC in LUTs across depth could have been due to high C inputs by roots through degradation (Rahman et al., 2021). The residue from leaf litterfall, which is the primary source of metabolites used by soil biota (Ares et al., 2010), could have increased SOC concentration at different depths.

The significant difference in SOC across LUTs was consistent with previous research in SSA (Kim et al., 2016; Muhati et al., 2018; Sommer et al., 2018; Kadiri et al., 2021). The SOC concentration under sole maize across all depths was below the critical limit (1.5%) as per Fairhurst. (2012). Low SOC under sole maize and sorghum corroborates with Degu et al. (2019), who reported low SOC concentration under continuous maize plantation compared to maize pepper-pepper. Additionally, the plant residue removal and low nutrient replenishment in the study area (Henry et al.,2009; Sommer et al., 2018) could have lowered the amount of carbon in soils. Frequent cultivation could have increased soil aggregate disturbance and microbial activities, thus reducing SOC concentration (Swanepoel et al., 2016). The amount of clay content difference could have led to varying levels of SOC (Sommer et al., 2018) in different LUTs. The SOC concentration under agroforestry L was significantly higher than monocrops LUTs (sole sorghum and sole maize, Figure 2.2). This corroborates the findings of several studies conducted in SSA (Henry et al., 2009; Kim et al., 2016; Namirembe et al., 2020). Guo et al. (2020) found significantly higher SOC under the metasequoia agroforestry system than in the poplar plantation. The addition of leaf litter fall by the *Leucaena leucocephala* could have created favourable conditions for biotic activities for SOC accumulation and utilization (Polasky et al., 2011). The highest amount of SOC under agroforestry L compared to agroforestry M could be ascribed to differences in species. Additionally, the difference could be due to the ability of agroforestry L to fix nitrogen that aids in building SOC (Negash et al., 2015)). Compared to grazing land, agroforestry has huge potential to store SOC (Abegaz et al., 2020). On the contrary, McNaughton et al. (1997) reported grazing land promotes nutrient cycling due to animal droppings and urine.

### 2.3.4 Soil organic carbon stock in different land utilization types and depths

The SOC stock across the different LUTs and depths ranged between 1283.4 to 27057 kg C ha$^{-1}$. There was a significant ($p$<0.0001) difference in carbon stock at 0-5 cm depth across all LUTs. The variation was between 6313.2 and 20069.7kg C ha$^{-1}$ (Figure 2.3). A significant ($p$<0.0001) difference was observed at 5-10cm depth that varied between 5411 and 17258 kg C ha$^{-1}$. At 10-20 cm depth, the SOC stock varied significantly ($p$<0.0001) across the LUTs with a range of 1283 to 26913 kg C ha$^{-1}$. There was also a significant ($p$<0.0001) difference in SOC stock at 20-30 cm. The lowest amount of SOC under sole maize (1283.47 kg C ha$^{-1}$) and highest amount of SOC under agroforestry L (26913.1kg Cha-1) were observed at 20-30 cm depth. Compared to all LUTs, agroforestry L had the highest carbon stock. The lowest SOC stock was detected under sole maize (Figure 2.4). Carbon stock increased with depths across the LUTs except in agroforestry L (Figure 2.3). There was an increasing carbon stock from 0-5 to 5-10 cm and decreasing from 10-20 to 20- 30 cm under agroforestry L. The variability of SOC stock differed significantly

($p$<0.00001) across LUTs.

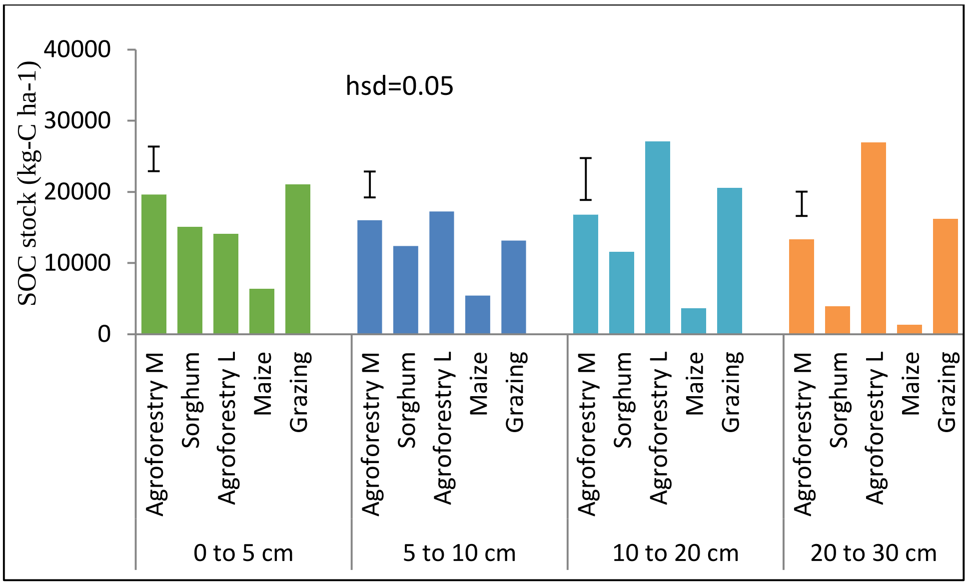


**Figure 2.3** Soil organic carbon (SOC) stock in different land utilization types (Agroforestry M= Agroforestry with *Markhamia lutea*, sole sorghum, Agroforestry L= Agroforestry with *Leucaena leucocephala*, sole maize and grazing land) at different depths in Siaya County, Kenya. a) SOC in % and b) SOC in g $kg^{-1}$ of soil ($p \leq 0.05$).

The estimated SOC stock between the LUTs was from 16631 to 85287kg $Cha^{-1}$ (Figure 2.4). There was high SOC stock in agroforestry L, while sole maize had the least SOC stock.

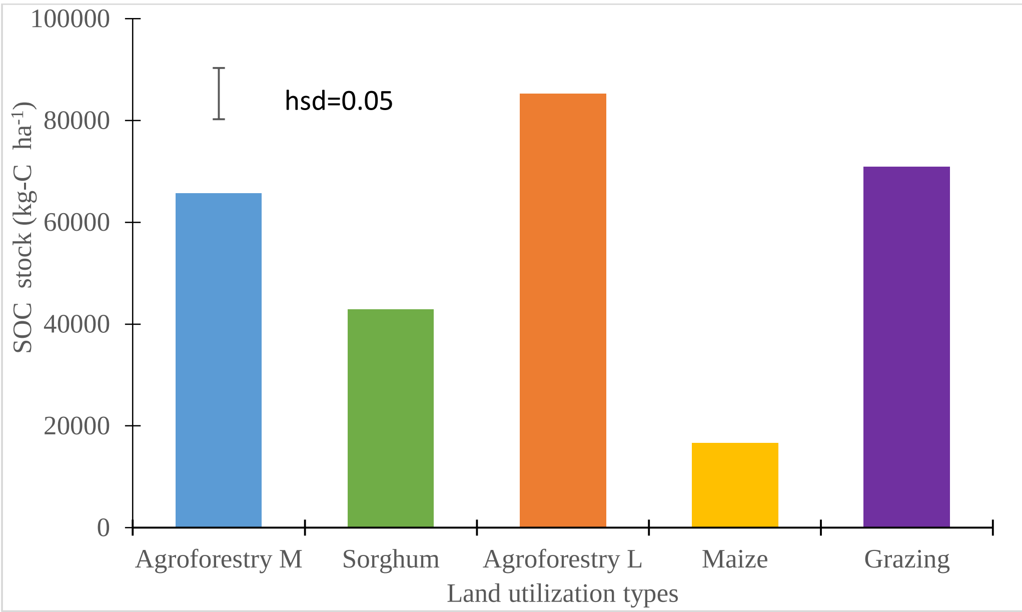


**Figure 2.4** Soil organic carbon stock (SOC) stock in different land utilization types (Agroforestry M= Agroforestry with *Markhamia lutea*, sole sorghum, Agroforestry L=

Agroforestry with *Leucaena leucocephala*, sole maize, and grazing land) at 0 to 30 cm depth in Siaya County, Kenya. ($p \leq 0.05$).

There were significant differences in SOC stock under different LUTs. The results were in conjunction with the previous findings in the study area by Henry et al. (2009) and Sommer et al. (2018) that observed a high SOC stock under improved agriculture. There was a decreasing SOC stock with increasing depth in agroforestry M, sole sorghum, grazing land, and sole maize, consistent with Kadiri et al. (2021) and Rahman et al. (2021). This phenomenon can be explained by the difference in OM. Under agroforestry L, continuous roots availability could have led to increasing SOC stock with increasing depth similar to the findings of Rahman et al. (2021). Conversely, the decreasing SOC stock with increasing depth under other LUTs could be ascribed to the decreasing OM with increasing depth. The results also agreed with Sa˜o Paulo, Brazil (Sarto et al., 2020), who reported decreasing SOC stock with increasing depth in Votuporanga city. Conversely, agroforestry L did not follow the trend due to low stock at 0-5cm depth compared to the5-10 and 10-20, 20-30cm depth. The high carbon under grazing land corroborated with the findings of McNaughton et al. (1997). This could be attributed to continuous root turnover that favored carbon accumulation (Sarto et al., 2020). However, some studies, such as Reszkowska et al. (2011) and Qiu et al. (2013), reported results contrary to the findings of this study. Qiu et al. (2013) found a carbon stock loss under grazed lands. Additionally, Abegaz et al. (2020) reported low carbon under grazing land compared to croplands.

Soils in agroforestry L showed significantly higher SOC stock than all LUTs due to the increasing supply of N by *Leucaena leucocephala*. These results were consistent with the findings of other studies conducted in SSA (Birch-Thomsen et al., 2007; Pardo et al., 2012; Muhati et al., 2018). Smith et al. (2008b) also showed high carbon stock under agroforestry systems. The addition of leaf litter residue from *Leucaena leucocephala* increased SOC stock by increasing microbial decomposition of labile organic matter (Lu et al., 2011). Additionally, root exudates and faunal bioturbation could have significantly increased SOC stock accumulation (Vesterdal et al., 2002). The difference in SOC accumulation under the two agroforestry (Agroforestry L and Agroforestry M) LUTs could be attributed to the difference in tree species. While agroforestry L is a leguminous plant, agroforestry M is non-leguminous hence difference in nitrogen levels that plays a fundamental role in building up SOC (Rahman et al., 2021).

Soils in croplands are characterized by low nutrients coupled with degradation (Kihara et al., 2015; Cavanagh et al., 2017) due to low nutrient replenishment (Kanyenji et al., 2020). Sole maize and sole sorghum in this study had low nutrient replenishment due to frequent cultivation that leads to soil OM, exposing the available carbon to the atmosphere. Also, cultivation could accelerate weathering and SOC oxidation (Smith et al., 2008), therefore, reducing inputs of organic matter to soil, and thus affecting the SOC stock levels (Sommer et al., 2018; Kanyeji et al., 2020). Researchers have reported low carbon stock under croplands in Western Kenya (Henry et al., 2009; Sommer et al., 2018). Additionally, crop residue removal during harvesting could be a fundamental reason for the low SOC stock under sole maize and sole sorghum. Abegaz et al. (2020) reported a drastic reduction in carbon stock under intense croplands compared to grazing lands. Also, plant pest damage coupled with decomposition of plant fragments in soil maize could have aggravated loss of carbon through heterotrophic process at the expense of terrestrial carbon inputs (Smith et al., 2008b).

### 2.3.6 Percentage distribution of SOC at different depths and land utilization types

There was high percentage carbon distribution under all LUTs at 0-5 cm depth except agroforestry L (Figure 2.5). The percentage SOC distribution in agroforestry L increase with increasing depth. The order of carbon distribution at 0-5cm depth was agroforestry L<grazing land<agroforestry M<Sole sorghum<Sole maize. There was 16.48% of SOC at 0-5 cm depth under agroforestry L. High SOC was observed at 20-30 cm depth under agroforestry L compared to all the LUTs. Sole maize had the highest carbon stock distribution (37.96%) at 0-5 cm depth. At 5-10 cm depth, the percentage distribution ranged between 32.5 to 18.6%. Sole maize had a high percentage at this depth compared in all LUTs. The range of carbon at 10-20 cm varied between 31.7% and 21.8%. Across the LUTs, a decreasing carbon distribution with increasing depth under sole maize and sole sorghum was detected. In contrast, carbon distribution under agroforestry L increased with increasing depth (Figure 2.5).

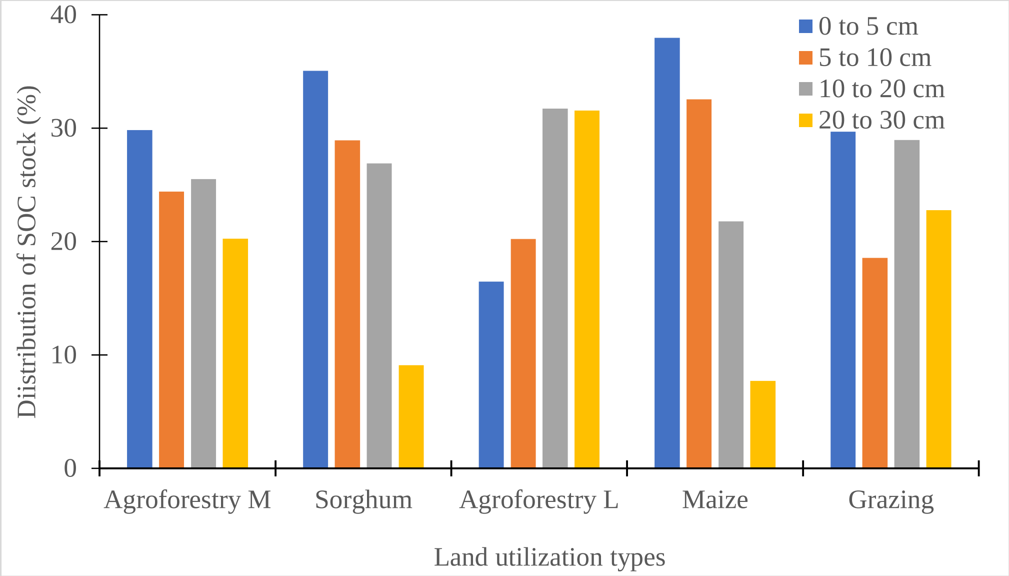


**Figure 2.5** Percentage distribution of SOC stock in different land utilization types (Agroforestry M= Agroforestry with *Markhamia lutea*, sole sorghum, Agroforestry L= Agroforestry with *Leucaena leucocephala*, sole maize and grazing land) at different depths in Siaya County, Kenya

The SOC stock distribution exhibited a significant difference across different LUTs and depths. Compared to all LUTs, agroforestry L had the lowest SOC stock distribution at 0-5 cm depth and high SOC stock at 20-30 cm depth. That could be ascribed to high root density that increases micropores (Sarvade et al., 2014), aiding the percolation of SOC inform of DOC to deeper depths. Tian et al. (2011) reported that high SOC stock distribution at 20-30 cm depth could have been due to high macro-faunal activities and root exudates that favour the build-up of SOC. The difference in SOC stock in the two agroforestry could be ascribed to the difference in rooting systems that aid in SOC accumulation (Negash et al., 2015). High SOC distribution at the upper depths under sole maize, sole sorghum, and grazing land could have been due to more organic matter than at deeper depths (Kadiri et al., 2020). Additionally, increased mineralization by soil biota could have contributed to huge SOC concentration at the superficial layer (Schmidt et al., 2011). There was a decreasing SOC stock distribution with increasing depth under sole maize and sorghum. There could have been differences in organic matter and soil texture across the soil profile (Bruun et al., 2010; Saidy et al., 2013).

### 2.3.7 Correlation between soil bulk density and SOC concentration

Soil bulk density correlated negatively with SOC across the LUTs except under grazing land (Table 2.2). The correlation between soil bulk density and SOC content significantly correlated positively (*p*=0.0001) with grazing land and negatively (*p*=0.0003) with agroforestry M.

**Table 2.2** Relationships between soil bulk density and SOC under different land utilization types

| LUTs | Coefficient | p-value |
|---|---|---|
| Agroforestry M | -0.868*** | 0.0003 |
| Sole sorghum | -0.138 | 0.7 |
| Agroforestry L | -0.140 | 0.7 |
| Sole Maize | -0.274 | 0.4 |
| Grazing land | 0.900*** | 0.0001 |

(** represents a significant correlation at P < 0.01, LUTs=Land utilization types, (Agroforestry M= Agroforestry with *Markhamia lutea*, sole sorghum, Agroforestry L= Agroforestry with *Leucaena leucocephala*, sole maize and grazing land) in Siaya County, Kenya

The SOC concentration showed a negative correlation with soil bulk density since soil porosity is a measure of soil productivity which is a function of SOM. Similarly, the amount of SOC is a determinant of the availability of micropores in soils (Tanveera et al., 2016). Results were in agreement with those of Rahman et al. (2020) and Eid et al. (2020), who reported a negative correlation of SOC with the soil bulk density. Blanco-Canqui et al. (2009) reported similar results despite the difference in the texture of soils. Compaction in grazing land by animal trampling could have reduced the cycling of labile carbon in soils after enrichment with animal droppings. Additionally, there could have been low percolation of DOC hence the high concentration of SOC with increasing bulk density (Chaudhari et al., 2013). Results from grazing land were in accord with Stavi et al. (2008), who reported a positive correction of SOC with soil bulk density.

The study demonstrated that LUTs influence SOC storage. The short time during which the study was conducted could have limited the influence of treatments on soil physicochemical properties. The benefits of agroforestry systems on carbon inputs could be more evident at a certain time scale. Nonetheless, the study fills a data gap in the contribution of smallholder farms' LUTs to carbon dynamics.

## 2.4 Conclusion

Results exhibited a difference in SOC stock across the LUTs and depths. Greater SOC stocks were detected under agroforestry L and grazing land. The type of agroforestry systems adversely affected SOC accumulation. Compared to agroforestry M, agroforestry L showed high SOC stock. The SOC concentration varied between depths and decreased with increasing depths in all LUTs except agroforestry L.

Additionally, soil bulk density was a predictor of SOC accumulation since there was a negative correlation between soil bulk density and SOC concentration. This study showed that agroforestry L is fundamental land utilization in carbon storage and helps in carbon buildup. In addition, grazing land showed promising results in carbon storage, thus limiting drastic climate change. This study shows the impacts of land utilization types on soil organic carbon. Therefore, there is a need to monitor soil organic carbon through quantification to inform on carbon dynamics. The diversity of land utilization types in Western Kenya causes soil organic carbon stocks variability. The SOC quantification offers an opportunity to increase carbon data inventories and carbon capture.

# CHAPTER THREE

## SOIL GREENHOUSE GAS EMISSIONS FROM DIFFERENT LAND UTILIZATION TYPES OF WESTERN KENYA


### Abstract

There is a vast data gap for the National and regional greenhouse gas (GHG) budget from different smallholders' land utilization types in Kenya and sub-Saharan Africa (SSA) at large. Quantifying soil GHG (methane $CH_4$, carbon dioxide $CO_2$, and nitrous oxide $N_2O$) emissions from different smallholders' land utilization types is essential in filling the data gap. Soil GHG emissions from different land utilization types in Western Kenya were quantified. The five land utilization types include 1) Agroforestry M (Agroforestry *Markhamia lutea),* 2) sole sorghum, 3) Agroforestry L (Sorghum and *Leucaena leucocephala),* 4) sole maize, and 5) grazing land. The soil GHG fluxes varied $CH_4$ ($p$<0.0001), $CO_2$ ($p$=0.001), and $N_2O$ ($p$<0.0001) across the land utilization types. Low $CH_4$ uptake under grazing land (-0.35 kg $CH_4$-C ha$^{-1}$) and the highest under sole maize -1.05 kg $CH_4$-C ha$^{-1}$ was observed. Low soil $CO_2$ emissions under sole maize, 6509.86, and e highest under grazing land, 14400.75 kg $CO_2$-C ha$^{-1}$ was observed. The results showed the lowest soil $N_2O$ fluxes under grazing land, 0.69 kg $N_2O$-Nha$^{-1,}$ and the highest under agroforestry L 2.48 kg $N_2O$-N ha$^{-1}$. The main drivers of soil GHG fluxes were soil bulk density, soil organic carbon, soil moisture, clay content, and root production. The yield-scale $N_2O$ fluxes ranged from 0.35 under sole maize to 4.90 g $N_2O$-N kg$^{-1}$ grain yields under Agroforestry L. The findings help in understanding the GHG dynamics across the LUTs.



**Keywords;** Land utilization types; soil-atmosphere exchange; Nationally Determined Contributions; Yield scaled $N_2O$ emissions

## 3.1 Introduction

Since the advent of the industrialization, the global concentration of soil greenhouse gas (GHG) fluxes has risen (Pachauri et al., 2014). The upsurging population and the need for more food have increased land intensification for improved crop production (Pachauri et al., 2014). Different land utilization types (LUTs) have varying soil GHG ($CH_4$, $CO_2$, and $N_2O$) fluxes potential (Tubiello et al., 2013; Valentini et al., 2014; Liang et al., 2016; Tongwane et al., 2016; Kim et al., 2016; Wachiye et al., 2021). Through fertilizer, manure, and crop residue, land utilization intensification could surge soil GHG fluxes in the quest for increased food production (Hickman et al., 2015; Macharia et al., 2020; Musafiri et al., 2020a). Despite GHG fluxes potential of different land utilization types on soil GHG fluxes, there is a lack of experimentally GHG flux data. Smallholder-based data that can inform Nationally Determined Contributions (NDCs) in most sub-Saharan Africa (SSA), including Kenya is required. Therefore, soil GHG measurements from common land utilization types among smallholder farmers in Kenya are essential to inform policy decisions and improve the National GHG reporting accuracy to United Nations Framework Convention on Climate Change (UNFCCC).

Soil acts as both sink and source of soil GHG fluxes (Pelster et al., 2017; Rosenstock et al., 2016). The overall soil-atmosphere exchange ($CH_4$, $CO_2$, and $N_2O$) results from a complex biogeochemical process (Butterbach-Bahl et al., 2013). The soil-atmosphere exchange across smallholders' land utilization types is controlled by various soil physiochemical properties, including bulk density, soil organic carbon, nitrogen, soil pH, soil moisture, and soil temperature (Pelster et al., 2017; Ortiz-Gonzalo et al., 2018; Wanyama et al., 2018). For improved productivity, land management practices such as tillage and soil amendments could trigger soil GHG fluxes (Macharia et al., 2020a). Climate factors, vegetation cover, and crop types across different utilization types significantly influence soil GHG fluxes (Rosenstock et al., 2016; Pelster et al., 2017). The diversified LUTs such as; grazed lands, agroforestry systems and intensively managed croplands (Abegaz et al., 2020; Wachiye et al., 2020), increase the soil GHG uncertainty (Ondier et al., 2020). The availability of the leguminous tree species (Kim et al., 2016) affect the quality and quantity of substrates that drive GHG emissions. Despite the potential contribution of different land utilization types in the National GHG budget and in informing the NDCs in Kenya (Wachiye et al., 2020), there is limited availability of farm-level data.

*Markhamia Lutea* is a non-leguminous and evergreen tree that belongs to a family of *Bignoniaceae*. It is the most widespread species of trees in Western Kenya and inputs up to 115.9 M g $ha^{-1}$ of carbon (Henry et al., 2009). Due to its economic viability, smallholder farmers use Markhamia in the agroforestry system. The amount of carbon input fixed by Markhamia could increase the substrate availability for microorganisms, thus increasing soil microbial activities. Additionally, the amount of C in soils could increase bioturbation and exudation of soil organic matter triggering $CO_2$ emissions (Wanyama et al., 2019). *Leucaena leucocephala* is evergreen and thornless tree belonging to the *Fabaceae* and *Mimosoideae* subfamily (Alemán-Ramirez et al., 2022). *Leucaena sp* accelerates nitrogen cycling, such as nitrification and denitrification. Leguminous trees could trigger emissions of $N_2O$ due to the high availability of N in soils (Ishizuka et al., 2021). The amount of N is a function of C, thus the risk of accelerating GHG emissions. Therefore, soil GHG fluxes measurements from smallholders' land utilization types are essential.

The objective of this study was to quantify soil greenhouse gas emissions of selected land utilization types of smallholder farms in Siaya County.

## 3.2 Materials and Methods

### 3.2.1 Study area

Soil greenhouse gas experimentation was conducted in a smallholder farm, with selected farm utilization types of interest, in Nyajuok sub-location, Siaya County, Western Kenya. The farm is approximately 1236 m above sea level and lies within the lower midland (LM1)- “sugarcane belt” agro-ecological zone. It receives bimodal rainfall with long rain (L.R.) season from March to July and short rain (S.R.) from August to December. The annual rainfall ranges between 1500 mm and 1900 mm, and average annual temperatures of 21.80 to 20.9°C. The long rain (L.R.) and short rain (S.R.) season rainfall amount range between 750 to 950mm and 600 to 800mm, respectively (Jaetzold et al., 2010). The highest temperatures are experienced from January to March. The area is suitable for maize (*Zea mays*), sorghum (*Sorghum bicolar*), common beans (*Phaseolus vulgaris*), cowpeas (*Vigna unguiculata*), sweet potatoes (*Ipomoea batatas*), soya beans (*Glycine max*), sunflower (*Heliuthus annuus*), spinach (*Spinacia oleracea*), and onions (*Allium cepa*) (Jaetzold et al., 2010). The soil type is Ferralsols, with inherent low soil fertility (Jaetzold et al., 2010). The low soil fertility constrains the implementation of cropping practices without amendments. The predominant primary land utilization types include grazing, agroforestry, maize, and sorghum (Jaetzold et al., 2010).

### 3.2.2 Experimental setup and management

The selection of the smallholder farm for the field experimentation was informed by the existence of the five LUTs of interest (Figure 3.1). The LUTs were (i) sorghum monocrop (ii) sorghum-agroforestry - *Markhamia lutea* (Agroforestry-M) (iii) sorghum-agroforestry *Leucaena leucocephala* (Agroforestry-L), (iv) maize monocrop, and (v) Grazing land. Under each LUT, three PVCs circular static chambers were installed to a 5 cm depth following Pelster et al. (2017).

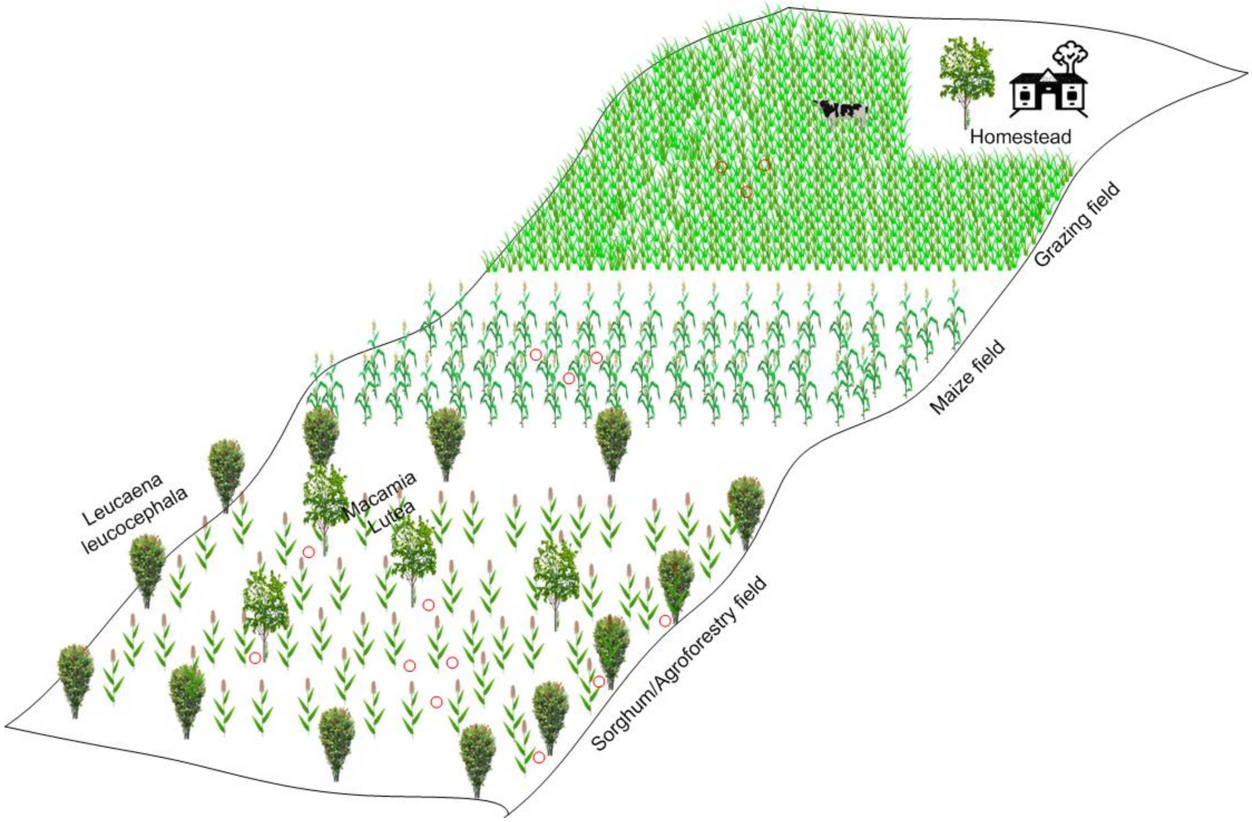


**Figure 3.1** Sketch representation of the smallholder farm, the five land utilization types, and chamber placement for gas sampling. The small red circles represent the static chambers (3 replicates per LUT).

**Table 3.1** Farm management practices in different land utilization types in Siaya County, Kenya

| LUTs[1] | Land preparation | Fertilization | Weeding |
|---|---|---|---|
| Agroforestry M | Disc ploughing with moldboard on 30th July 2020 & ox-ploughing on 23rd February 2021 | Manure broadcasting across the two seasons. 6th August 2020; manure, 2tha$^{-1}$, DAP 112kg/ha, 14th April 2021; manure, 2tha$^{-1}$ DAP 125 kg/ha | 28th September 2020 & 30th April 2020 |
| Sole sorghum | Disc ploughing 30th July 2020 & Ox-ploughing 20th on February 2021 | Manure broadcasting across the two seasons. 6th August 2020; manure, 2tha$^{-1}$, DAP 112kg/ha, 14th April 2021; manure, 2tha$^{-1}$ DAP 125 kg/ha | 28th September 2020 & 30th April 2020 |
| Agroforestry L | Disc ploughing 30th July 2020 &Ox-ploughing on 10th March 2021 | Manure broadcasting across the two seasons. 6th August 2020; manure, 2tha$^{-1}$, DAP 112kg/ha, 14th April 2021; manure, 2tha$^{-1}$ DAP 125 kg/ha | 30th September 2020 & 30th April 2020 |
| Sole maize | Ox-ploughing 8th August 2020 & on 16th February 2021 | 14th September 2020; manure, 2tha$^{-1}$, DAP 112kg/ha, 29th March 2021; manure, 2tha$^{-1}$ | 2nd October 2020 & 18th April 2020 |

| | | | |
|---|---|---|---|
| | | DAP 125 kg/ha | |
| Grazing land[2] | - | - | - |

[1] LUTs is the land utilization types i) Agroforestry M (Agroforestry *Markhamia lutea* and sorghum*)*, ii) sole sorghum (sorghum monocrop), iii) Agroforestry L (Sorghum and *Leucaena leucocephala)*, iv) sole maize (maize monocrop), and iv) grazing land.

[2] No crop planted in the grazing land

All field management practices during the experimental period were observed and recorded under all LUTs except grazing land. They included ploughing, manure application, fertilization, planting weeding, and harvesting. During the short rain season (S.R. 20), land preparation was done using a tractor, followed by ox-ploughing. However, primary and secondary tillage was implemented using ox-plow during the long rain season (L.R. 21). Additionally, plant residue was retained in sole sorghum, agroforestry M and agroforestry L during S.R. 21. Animal manure was incorporated two weeks before planting in each cropping season. The manure (nitrogen content of 1.09%) was applied at a 2 tons per hectare rate, while inorganic fertilizer application was done during planting. Sorghum planting and fertilizer; Diammonium phosphate (DAP) applications were done on Aug 14$^{th}$ 2020, and Apr 2$^{nd}$ 2021. The rate of DAP applied varied; during S.R., the rate was 112kg/ha (approximately Less than 23 kg N ha$^{-1}$), while during L.R., the rate was 125 kg/ha (approximately less than 25 kg N ha$^{-1}$), in the sole sorghum, agroforestry-M, and agroforestry-L. The sorghum spacing was 75 cm by 20 cm inter-rows and intra-rows, respectively. Maize planting and fertilizer; Diammonium phosphate (DAP) application on the sole maize LUT was done on Sept 7$^{th}$, 2020, and Mar 29$^{th}$, 2021 during S.R. 20 and L.R. 21. The maize spacing was 75 cm (inter-rows) and 50 cm (intra-rows). Weed management was implemented twice during each cropping season using a hand hoe. There was flooding in the sole sorghum, Agroforestry-M, and Agroforestry-L between March and May 2021. The flooding coupled with Striga weed (*Striga hermonthica*) infestation suppressed sorghum yields. The S.R. 20 was from July 2020 (harvest of the previous crop) to December 2020 (harvesting), while the L.R. 2020 ran from January 2021 (the following harvesting) to June 2021.

### 3.2.3 Soil GHG fluxes measurements and analysis

Three PVC circular vented static chambers for soil GHG fluxes ($CO_2$, $CH_4$, and $N_2O$) sampling were installed each LUT (Figure 3.1) at the onset of the experiment. Each chamber was composed of a lid (20 cm by 8 cm diameter and height) and a base (20 cm by 10 cm, diameter, and height, with 3 cm above the ground and 7 cm below ground). The lid was fitted with a sampling rubber septum and a vent for maintaining pressure equilibrium between the atmospheric pressure. The top was equipped with rubber to ensure airtight sealing during sampling headspace. The chambers remained undisturbed during the study period, except during major land management operations such as land preparation, manure application, fertilization, and planting. During such events, the chambers were removed and re-installed immediately after. Chambers at the grazing land were not removed during the entire study period.

The soil GHG flux measurements were conducted weekly during the rainy periods and biweekly during the dry periods following static chamber technique. Additionally, soil GHG flux measurements were done following key field management activities such as ploughing, manure or fertilizer application, planting, and rainfall (Macharia et al., 2021; Musafiri et al., 2021). For consistency, two casual laborers were recruited and trained on soil GHG sampling at the onset of the experiment. The chamber base and lid were held airtight using the circular rubber band during each sampling event. Soil GHG samples were collected between 0800 and 1200 hours; the time considered representative of the diurnal temperature thus limiting variation in flux patterns (Parkin et al., 2012). During each sampling event, 60 ml of gas was sampled from each chamber using a 60 ml capacity syringe fitted with a Luer-lock and injected into a label, pre-evacuated 20 ml glass vial. The soil GHG samples were collected at 0-, 10-, 20-, and 30-min intervals. The gas samples were transported to Mazingira Laboratories (the International Livestock Research Institute) for analysis.

The soil $CO_2$, $CH_4$, and $N_2O$ concentrations were analyzed using SRI 8610C gas chromatography (G.C). The G.C. was tailored with a flame ionization detector (FID) for

$CH_4$ and $CO_2$ emissions and a $^{63}$Ni-electron capture detector (ECD) for $N_2O$ (with pure N as a carrier gas). The G.C. was calibrated after every four samples using a known $CO_2$, $CH_4$, and $N_2O$ concentration. The relationship between peak area and concentration over the 30 min headspace was used to determine the soil GHG fluxes. Since FID assumes linear function upon chamber closure, the $CO_2$ and $CH_4$ concentrations were calculated using linear regression (Musafiri et al., 2020a). Nonlinear and power functions between $N_2O$ mass and time were used to calculate soil $N_2O$ concentration since the ECD assumes a nonlinear power function between time and $N_2O$ masses (Macharia et al., 2020).

### 3.2.4 Soil GHG fluxes calculation

The soil GHG fluxes were calculated by accounting for environmental factors, including air pressure and temperature, following the ideal gas law (Musafiri et al., 2020a) following Equation 3.1.

$$\text{Fghg} = \frac{\text{b}\times\text{Mw}\times\text{Vch}\times 60\times 10^{6}}{\text{Ach}\times\text{Vm}\times 10^{9}} \qquad \text{(Equation 1)}$$

Where Fghg is the flux rate, b is the slope of increase/decrease in concentration, Mw is the molecular weight of component (g $mol^{-1}$), VCh is chamber volume ($m^3$), ACh is chamber area ($m^2$), Vm is the corrected standard gaseous molar volume ($m^3$ $mol^{-1}$) given by Equation 2.

$$\text{Vm} = 22.4\times 10^{-3}\ \text{m}^3\ \text{mol}^{-1}\times\frac{273.15+\text{Temp}}{273.15}\times\frac{\text{air pressure}}{1013} \qquad \text{(Equation 2)}$$

The quality of gas concentration was checked using $R^2$ of $CO_2$ concentration. For validation and reliability of the GHG concentration, the fourth sampling interval data was discarded in the event of $R^2<0.90$ for $CO_2$ as fluxes were assumed to have experienced leakage. However, upon discarding the fourth sampling interval and the $R^2$ were still less than 90%, the assumption was made that there was contamination, and that dataset was discarded for analysis. The minimum detection limits were computed for both linear and nonlinear models following Parkin et al. (2012) for $CH_4$, $CO_2$, and $N_2O$ emissions at ±0.03 and ±0.08 $CH_4$-C mg $m^{-2}$ $h^{-1}$, 2.87 and 9.52 mg $CO_2$-C $m^{-2}$ $h^{-1}$, and ±3.16 and ±9.90 µg$N_2O$-N $m^{-2}$

$h^{-1}$. There was both negative and positive soil-atmosphere $CH_4$ and $N_2O$ exchange, indicating that the soils acted as both sources and sinks $CH_4$ and $N_2O$. The soil-atmosphere $CO_2$ balances were always positive, indicating that the ground was the net source of $CO_2$. The cumulative $CH_4$, $CO_2$, and $N_2O$ emissions were computed for each LUT replicate using linear interpolation between sampling days based on trapezoidal rule, following Barton et al. (2015).

### 3.2.5 Soil and weather monitoring

Soil samples were collected at 0-20 cm depth for soil organic carbon, bulk density, and soil texture analysis using a 5 cm diameter and 5 cm height core ring (Eijkelkamp Agrisearch Equipment, Giesbeek, The Netherlands). Four samples were collected from every LUT totaling to sixty samples. Samples were mixed for soil texture analysis to form one composite sample in every LUT, totaling five samples. The soil samples were analyzed following Okalebo et al. (2002). For soil organic carbon determination, Walkley-Black method was used. The soil samples were oven-dried at 105°C for 24 hours for soil bulk density determination. The soil bulk density was determined gravimetrically following Okalebo et al. (2002). Soil texture was determined using the hydrometer method (Okalebo et al., 2002). Rainfall data was collected using a manual rain gauge installed in the study area. Samples for soil moisture content determination were collected at 0-5cm depth during the soil GHG sampling events. Soil moisture was determined by oven drying at 105°C for 24 hours, and moisture was determined gravimetrically. Chamber temperature and soil temperature was also measured using a thermometer (TFA thermometer, Zum Ottersberg, Wertheim, Germany).

### 3.2.6 Crop yields and yield-scaled $N_2O$ emissions

Plot of 3 m by 3 m plot dimensions across the LUTs except for the grazing land to were used to estimate crop grain yields. Three subplots were selected to estimate crop yields in each land utilization type. Four planting holes (8 plants) were sampled to determine crop biomass. The wet weight of the crop harvested was determined using an electronic balance. The roots, leaves, stems, and grains sub-samples were air-dried for three weeks and oven-dried the subsamples at 60°C for 48 hours. The sub-samples were weighed after drying and converted the yields to kg $ha^{-1}$. The grain yields for both maize and sorghum were reported at 12.5% moisture content following Ngetich et al. (2014). The soil $N_2O$ fluxes (g$N_2O$-N$ha^{-1}$) was divided with the grain yields (Kg $ha^{-1}$) to determine the yield-scaled $N_2O$ emissions following Musafiri et al.(2020a).

### 3.2.7 Statistical analysis

The GHG data were subjected to analysis of variance (ANOVA) using SAS 9.4 software. Before analysis, the normality of soil GHG fluxes was tested using the Shapiro-Wilk test. The soil $N_2O$ fluxes were not normally distributed; thus, they were log-transformed. The influence of the land utilization types, seasons, and replicates on soil GHG fluxes were tested using a mixed linear model. Land utilization types were used as fixed effects and replicates and seasons as random factors. The Pearson's correlation was performed to test the relationship between soil GHG fluxes and soil bulk density, soil organic carbon, clay content, soil temperature, soil moisture, and roots.

## 3.3 Results and discussion

### 3.3.1 Soil and weather data

There was high soil bulk density, 1.53 g $cm^{-1}$ under grazing land, and the lowest 1.20 under agroforestry L (Table 3.2). The soil organic carbon varied significantly ($p<0.0001$) among the land utilization types (Table 3.2). There was high soil organic carbon, 2.23% under agroforestry M and the lowest 0.60% under sole maize. The soil texture was loam across different land utilization types (Table 3.2).

**Table 3.2** Baseline soil properties under different land utilization types at 0-20 cm depth in Siaya County, Kenya

| LUTs[1] | Bulk density (g $cm^{-3}$), n=3) | Soil organic carbon (%), n=3) | Soil pH (n=1) | Soil texture (%) | | |
|---|---|---|---|---|---|---|
| | | | | *Sand* | *Clay* | *Silt* |
| Agroforestry M | $1.23^{c}$ | $2.23^{a}$ | 5.2 | 47 | 19 | 34 |
| Sole sorghum | $1.40^{b}$ | $1.50^{b}$ | 4.9 | 48 | 15 | 37 |
| Agroforestry L | $1.20^{c}$ | $2.07^{a}$ | 5.4 | 46 | 18 | 36 |
| Sole maize | $1.50^{a}$ | $0.61^{c}$ | 4.8 | 52 | 18 | 30 |
| Grazing land | $1.53^{a}$ | $2.01^{a}$ | 5.1 | 50 | 18 | 32 |
| *P* value | <0.0001 | <0.0001 | | - | - | - |

[1] LUTs is the land utilization types i) Agroforestry M (Agroforestry *Markhamia)*, ii) sole sorghum (sorghum monocrop), iii) Agroforestry L (*Leucaena leucocephala)*, iv) sole maize (maize monocrop), and iv) grazing land.
[2] Mean bulk density and soil organic carbon with the same superscript in the same column during the season are not significantly different between land utilization types at p ≤0.05.

The average soil water content at 0-5cm depth across the land utilization types during the study period was 0.24 g $g^{-1}$ soil (Agroforestry M), 0.22 g $g^{-1}$ soil (sole sorghum), 0.22 g $g^{-1}$ soil (Agroforestry L), 0.15g $g^{-1}$ soil (sole maize), and 0.19g $g^{-1}$ soil (grazing land) (Figure 3.2c,3.3c,3.4c). The highest average soil moisture was observed under Agroforestry M and the lowest under sole maize. The cumulative seasonal rainfall was 727.60 mm and 737.00 during the SR20 and LR21 (Figure 3.2a,3.3a,3.4a). During the study period, the overall cumulative rainfall amount was 1465 mm. The overall rainfall was consistent with the long-term average rainfall in the study area, ranging between 800 mm to 1900 mm (Jaetzold et al., 2010).

### 3.3.2 Soil GHG

### 3.3.3 $N_2O$ fluxes

There was both negative and positive soil $N_2O$ fluxes across land utilization types throughout the study periods. The soil $N_2O$ fluxes ranged from -19.08 to 158.18 ųg $N_2O$-N $m^{-2}$ $h^{-1}$ (Figure 3.2b). High $N_2O$ fluxes was observed following precipitation events. The soil $N_2O$ fluxes were mainly positive, but there was few soil $N_2O$ uptakes, especially during the off-season.

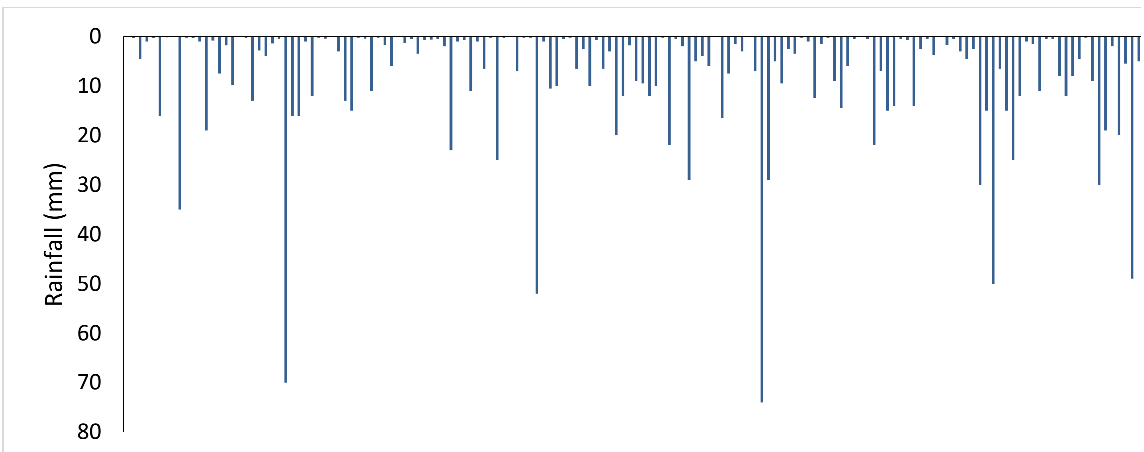


(a)

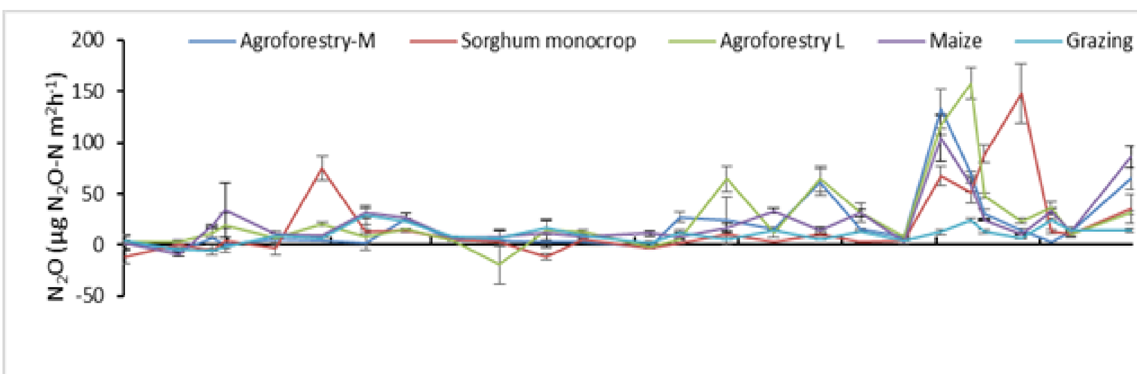




(b)

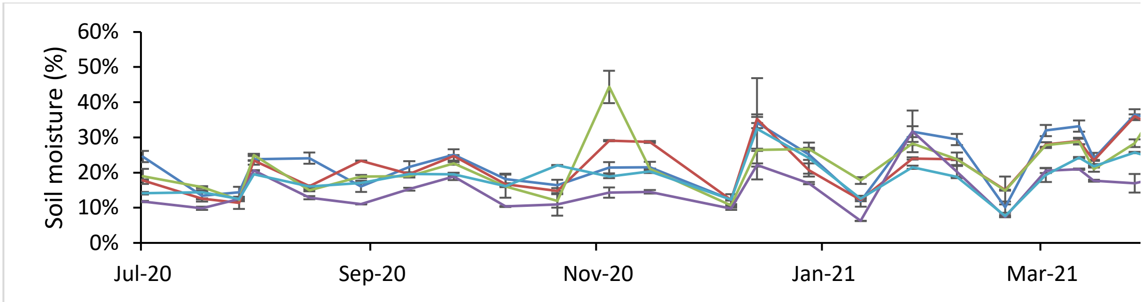


(c)

**Figure 3.2** a=Rainfall (mm), b=Soil Nitrous oxide (µg$N_2O$-N $m^{-2}$ $h^{-1}$), and c=soil moisture (%) in different land utilization types in Siaya County Kenya.

The soil $N_2O$ results from this study is consisted with other studies conducted in e range of the previous studies in East Africa (Rosentock et al., 2016; Pelster et al., 2017; Ortiz-Gonzalo et al., 2018; Musafiri et al., 2020a) that found a range of $N_2O$ fluxes from -20.00 to 200 ųg $N_2O$-C $m^{-2}$ $h^{-1}$ in maize crop under similar conditions. Grazing land also resulted to $N_2O$ emission of up to 150 ųg $N_2O$-C $m^{-2}$ $h^{-1}$, which was similar to the findings of Ortiz-Gonzalo et al. (2018) who found range of emissions from 20 to 500 ųg $N_2O$-C $m^{-2}$ $h^{-1}$ in the pasture land due to application of dung (mixture of dung and urine). There were instances of uptake of $N_2O$ similar to the findings of (Musafiri et al., 2020b) and Macharia et al., 2020), this phenomenon can be ascribed to reduction on the soil moisture which a function of precipitation. Generally, low moisture content favors uptake of $N_2O$ in soils (Butterbach-Bahl et al., 2013). The SSA smallholder farms received low N inputs (Ortiz-Gonzalo et al., 2018). The daily N2O reached peaks during high rainfall events that could be explained by the difference in soil moisture difference and increase in soil respiration. The onset of rains that coincided with planting and fertilization offered ideal conditions for nitrification and denitrification processes due to reduced oxygen availability limits microbial activity (Butterbach-Bahl et al., 2013). The four LUTs were applied with animal manure (see Table 3.1) which is the controlling factor in $N_2O$ emissions by increasing the availability of labile carbon. Hickman et al. (2014) found an increase in $N_2O$ fluxes by 58% from the fertilized chambers upon application of manure compared to unfertilized plots under *Zea mays* in Siaya. The availability of water in soil micropores coupled with availability of carbon from manure increases the $N_2O$ emissions unless saturation is reached. Even though there was data on different levels of soil saturation, Wanyama et al. (2018) reported that production of $N_2O$ is produced until soil saturation is reached where $N_2O$ is consumed due to limitation of oxygen in soils. Also, the availability of dung and urine deposition under grazing land could have led to increase in $N_2O$ emissions upon soil rewetting. Mineralization in soil leads to production of $N_2O$ (Liang et al., 2016). Therefore, the peaks under grazing land could be explained by availability of dung on grasses. Generally, the key events that elaborates $N_2O$ peak are high precipitation, increasing soil moisture content and fertilizer application. Macharia et al. (2020) and Musafiri et al. (2020b) found that $N_2O$ impulse is due to major events as listed earlier.

Under grazing land, the peaks can be explained by animal dung and urine deposition (Ortiz-Gonzalo et al., 2018). The availability of dung and urine increases their interaction with the soil biota during infiltration in the soil compartments. Zhu et al. (2018) reported that nitrous emissions correlate linearly with the amount of dung deposited on grasses.

### 3.3.4 $CH_4$ fluxes

The soil $CH_4$ fluxes were generally negative across the land utilization types with the highest uptake of -200.00 ųg$CH_4$-C $m^{-2}$ $h^{-1}$ (Figure 3.3). The soil $CH_4$ fluxes were mainly lower than the detection limit between -0.01 and +0.01 ųg$CH_4$-C $m^{-2}$ $h^{-1}$ across land utilization types. However, sporadically positive soil $CH_4$ fluxes were observed with the highest of 60 ųg $CH_4$-C $m^{-2}$ $h^{-1}$.

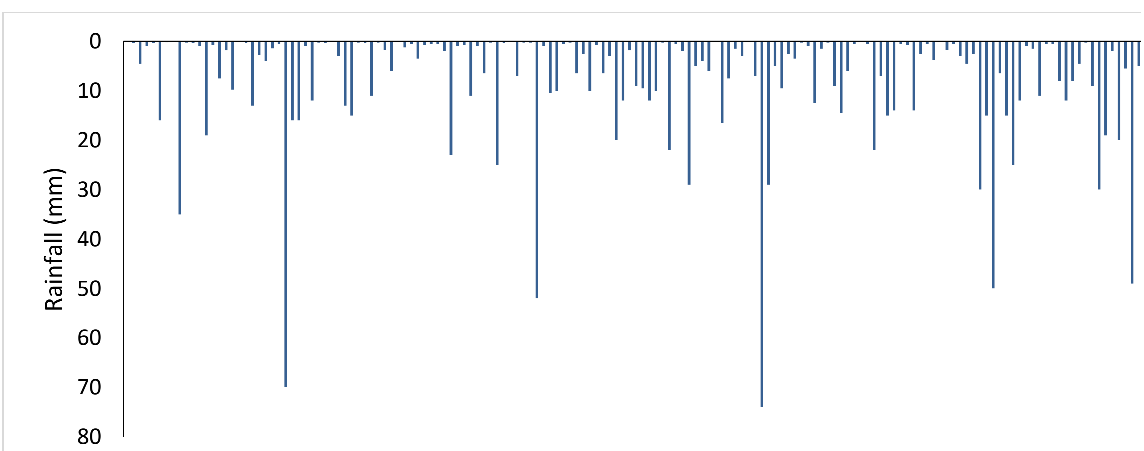


(a)

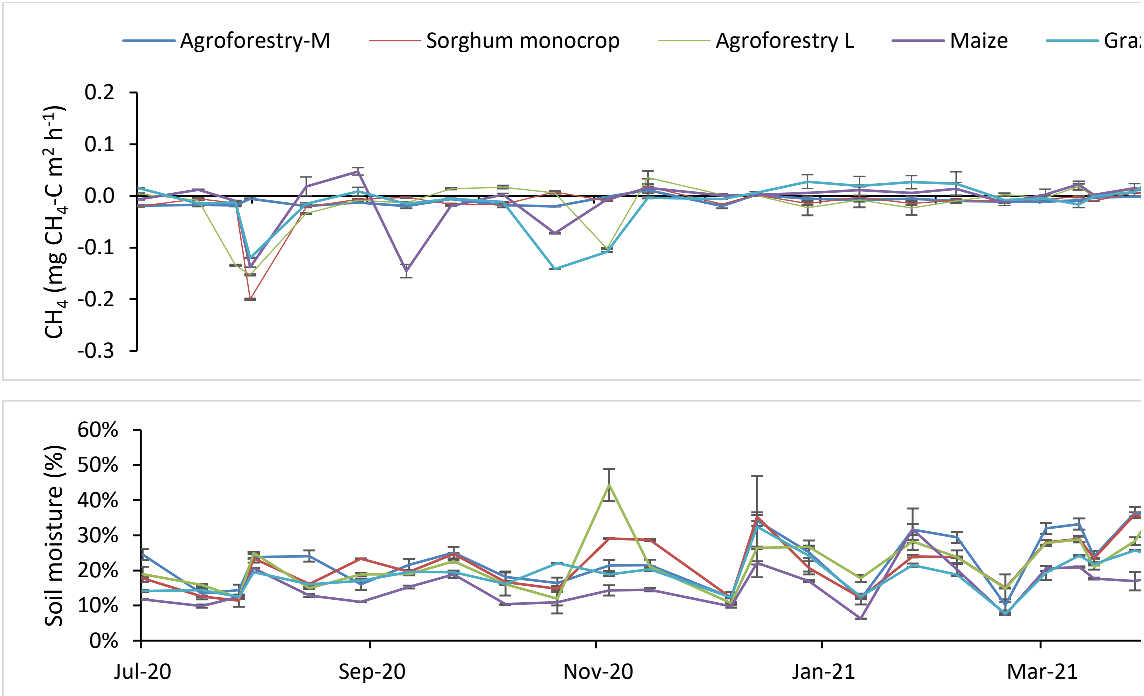


(b)

**Figure 3.3** a=Rainfall (mm), b=Methane ($CH_4$-C mg $m^{-2}$ $h^{-1}$), and c= soil moisture (%) in different land utilization types in Siaya County Kenya.

Soils acted as $CH_4$ sinks and source during the study period. These results were similar to the findings conducted in East Africa (Rosentock et al., 2016; Pelster et al., 2017; 2016; Musafiri et al., 2020a) that found a range of 0.02 to -60 CH4-C $m^{-2}$ $h^{-1}$ in smallholder croplands under similar condition. There was low methane production during dry period due to high rate of gas diffusivity and favorable aerobic conditions for methane uptake (Dutaur and Verchot, 2007). However, during the onset of rainfall, which led to an increase in moisture content, the $CH_4$ uptake became low reflecting the effects of moisture on $CH_4$ fluxes.

### 3.3.5 $CO_2$ fluxes

The soil $CO_2$ emissions ranged from 38.98 to 483.92 mg$CO_2$-C $m^{-2}$ $h^{-1}$ across the LUTs (Figure 3.4b). Low $CO_2$ emissions was observed on July 20 and Jan 21 across the LUTs. The $CO_2$ emissions was low under sole maize and sole sorghum compared to grazing land. There were also high $CO_2$ emissions following precipitation events through the study periods. Compared to all the LUTs, agroforestry M had the highest peaks following precipitation events.

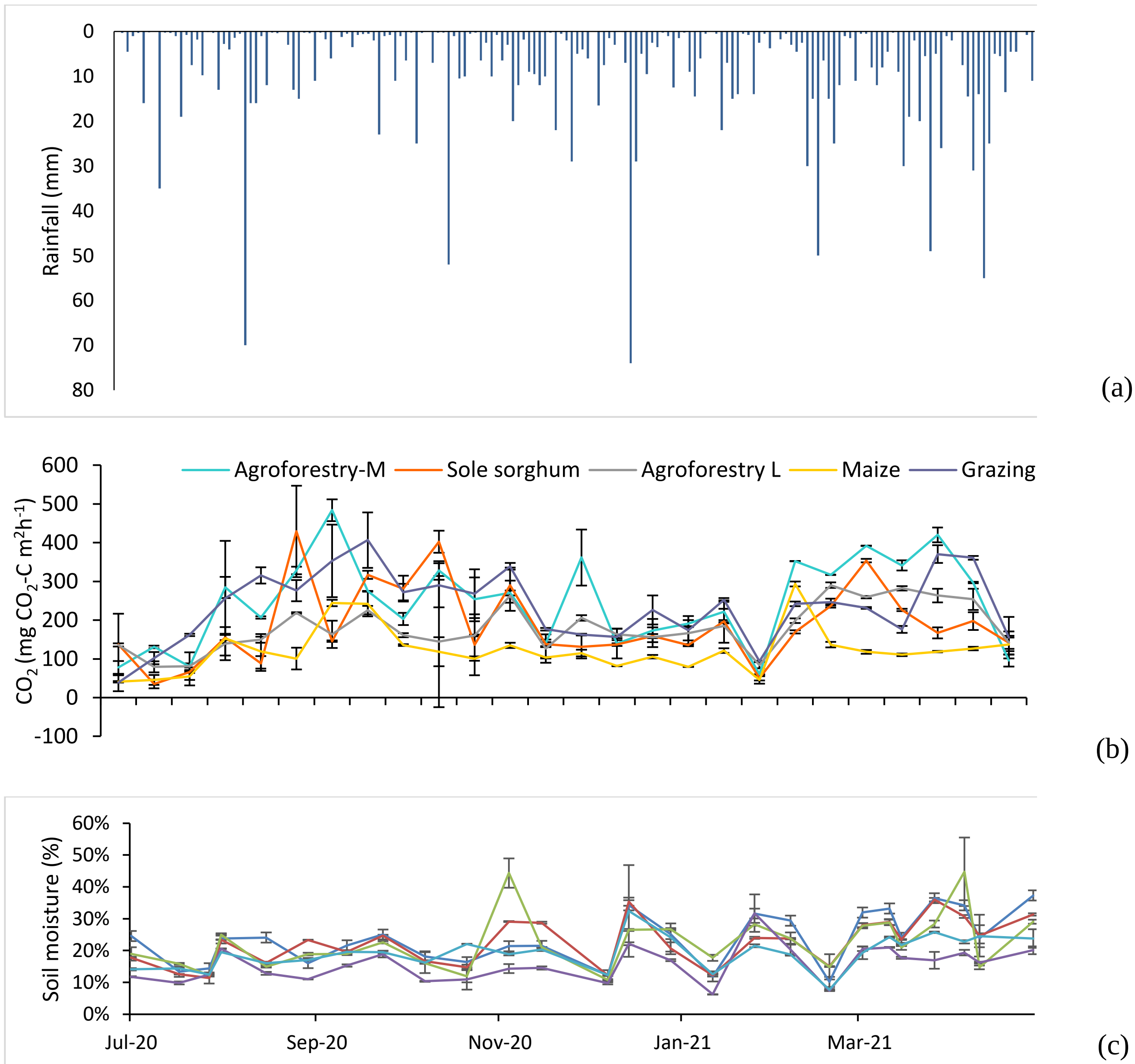


**Figure 3.4** a=Rainfall (mm), b=soil Carbon dioxide ($CO_2$-C $m^{-2}$ $h^{-1}$), and c=soil moisture (%) in different land utilization types in Siaya County Kenya.

There was an increased in soil $CO_2$ emission on onset of the precipitation across the LUTs. These observations are similar to the findings from SSA (Rosenstock et al., 2016; Wanyama et al., 2019; Wachiye et al., 2020) that found a range of 30 to 400 $mgCO_2$-C $m^{-2}$ $h^{-1}$ under different land use types under similar conditions. In addition, Pelster et al. (2017) and Musafiri et al. (2020) reported similar findings to these results following major events such ploughing, planting and fertilization in the smallholder farms. Generally, farm management practices (Pelster et al., 2017; Macharia et al., 2020) coupled with soil humidity perturbation, affects both soil biotic and abiotic factors. An influence on soil microclimate affects bio-faunal activities that drive carbon in soil thus soil $CO_2$ emissions. Therefore, farm activities such as fertilization (Ortiz-Gonzalo et al., 2018), which coincided with precipitation across different LUTs explains high pulse $CO_2$ emissions. For the case of grazing, there was high pulse $CO_2$ emissions during first precipitation which ca be elaborated by the rewetting of animal droppings thus causing Birch effect. However, there was instances of low $CO_2$ emissions due to low moisture content which is the function of precipitation. Also, during the study period, there was periods with no plants in the field except grazing land. Therefore, it is imperative to note the contribution of plants in respiratory processes, such as root respiration that is likely to increase soil $CO_2$ emissions (Rosenstock et al., 2016).

### 3.3.6 Cumulative GHG fluxes

The cumulative seasonal soil GHG emissions (CH4, CO2, and N2O) significantly varied across the land utilization types (Table 3.3). Highest $CH_4$ uptakes observed under sole maize (38% more compared to all LUTs during S.R. 20 and L.R. 21. There was lowest CH4 uptakes under agroforestry L and sole sorghum m during S.R. 20. During L.R. 21, there was 40% more $CH_4$ uptake under agroforestry L. We observed 30% and 36% more N2O emissions under agroforestry L than all the LUTs during SR 20 and LR 21 respectively. However, 13% less $N_2O$ emissions was observed under agroforestry M compared to all the LUTs during SR 21. Grazing land emitted high $CO_2$ (29 and 25% during SR 20 and LR 21 respectively), compared to other LUTs. There was significant seasonal differences ($P<0.0001$) and seasonal interactions ($P<0.0001$) during the study.

Annual cumulative soil GHG emissions varied across the land utilization types (Table 3.3). The $CH_4$ uptake under sole maize was 75% more compared to grazing land. Soil $CO_2$ emissions was 69% more in grazing land compared to sole maize. Conversely, grazing land emitted 22% less $N_2O$ than the agroforestry L.

**Table 3.3** Soil greenhouse gas emissions (Mean±SEM) as influenced by land utilization types between July 2020 and May 2021 in Siaya County, Kenya.

| Season[1] | LUTs[2] | CH4 fluxes (kg CH4-C $ha^{-1}$) | CO2 emissions (kgCO2-C $ha^{-1}$) | N2O fluxes (kgN2O-N$ha^{-1}$) |
|---|---|---|---|---|
| SR 2020 | Agroforestry M | $-0.43^{a}\pm0.01$ | $6347.52^{ab}\pm168.25$ | $0.26^{c}\pm0.02$ |
| | Sole sorghum | $-0.42^{a}\pm0.01$ | $6208.58^{bc}\pm344.15$ | $0.40^{bc}\pm0.02$ |
| | Agroforestry L | $-0.23^{a}\pm0.05$ | $5108.25^{cd}\pm551.70$ | $0.58^{a}\pm0.01$ |
| | Sole Maize | $-0.87^{b}\pm0.03$ | $3967.88^{d}\pm620.55$ | $0.43^{ab}\pm0.03$ |
| | Grazing land | $-0.34^{a}\pm0.09$ | $8949.50^{a}\pm515.86$ | $0.29^{bc}0.05$ |
| | P-value | 0.001 | 0.0001 | 0.002 |
| LR 2021 | Agroforestry M | $-0.20^{c}\pm0.01$ | $5367.04^{ab}\pm129.41$ | $1.28^{b}\pm0.06$ |
| | Sole sorghum | $-0.004^{b}\pm0.01$ | $4110.33^{c}\pm209.15$ | $0.69^{cd}\pm0.05$ |
| | Agroforestry L | $-0.26^{d}\pm0.01$ | $4423.09^{bc}\pm419.20$ | $1.90^{a}\pm0.11$ |
| | Sole Maize | $-0.18^{a}\pm0.01$ | $2541.98^{d}252.01$ | $1.00^{bc}\pm0.06$ |
| | Grazing land | $-0.005^{b}0.01$ | $5451.25^{a}\pm382.33$ | $0.40^{d}\pm0.06$ |
| | P-value | <0.0001 | 0.0001 | <0.0001 |
| Cumulative | Agroforestry M | $-0.63^{d}\pm0.01$ | $11714.56^{ab}\pm110.76$ | $1.54^{b}\pm0.06$ |
| | Sole sorghum | $-0.42^{b}\pm0.06$ | $10318.91^{bc}\pm931.05$ | $1.09^{c}\pm0.02$ |
| | Agroforestry L | $-0.49^{c}\pm0.04$ | $9531.34^{c}\pm948.53$ | $2.48^{a}\pm0.11$ |
| | Sole Maize | $-1.05^{e}\pm0.26$ | $6509.86^{d}\pm561.37$ | $1.43^{b}\pm0.5$ |
| | Grazing land | $-0.35^{a}\pm0.09$ | $14400.75^{a}\pm1210.88$ | $0.69^{c}\pm0.07$ |
| | P-value | <0.0001 | 0.001 | <0.0001 |
| | Seasonal *p* vaue[4] | <0.0001 | <0.0001 | <0.0001 |
| | Season*LUT[5] | <0.0001 | <0.0001 | <0.0001 |

[1] Season S.R. 2020 is short rains 2020, L.T. 2021 long rains 2021, and cumulative is the summation of the two seasons

[2] LUTs is the land utilization types i) Agroforestry M (Agroforestry *Markhamia lutea* and sorghum*)*, ii) sole sorghum (sorghum monocrop), iii) Agroforestry L (Sorghum and *Leucaena leucocephala)*, iv) sole maize (maize monocrop), and iv) grazing land.

[3] Average soil GHG emissions with the same superscript in the same column during the season are not significantly different between land utilization types at p ≤0.05.

[4] Seasonal P-value indicates soil GHG emissions difference between the two seasons.

[5] Season*LUT indicates fixed factor (land utilization types) interaction on soil GHG emissions with replicates and season as random factors.

The soil acted as a net sink of $CH_4$ fluxes. The cumulative soil $CH_4$ uptake ranged from -0.21 to -0.68 kg $CH_4$-C $ha^{-1}yr^{-1}$ consistent with previous studies in East Africa (Macharia et al., 2020; Musafiri et al., 2020a) under similar conditions in the smallholder farms. The difference in soil $CH_4$ uptake in this study could be ascribed to different management practices across the LUTs such as manure and tillage, which has huge impact on the soil organic that acts as substrates in soils for methanogenic archaea. Sole maize had high $CH_4$ uptake due to low SOC (see Table 3.2). Soil bulk density is among factors that controls $CH_4$ fluxes. Generally, soil bulk density is a function of soil porosity thus predicting diffusivity rate. Agroforestry M had a high $CH_4$ uptake, which could be explained by low soil bulk density (Table 3.2) that increases on gas diffusivity rate (Chi et al., 2016). The high $CH_4$ uptake in the agroforestry M could be attributed high diffusivity rate due to low soil bulk density coupled with high porosity. On the contrary, during SR 2020 there was low $CH_4$ uptake under agroforestry M due to flooding that could have created anaerobic conditions suitable for methane production. Soil $CH_4$ uptake under agroforestry L could be elaborated by the low soi bulk density. Also, even though there was not measure mineral N, leucacena leucocephala could have fixed nitrogen in soils. Thus, increasing $NH_4$+-N gradient hence competing for the mono-oxygenase enzyme which accelerates $CH_4$ oxidation. According to a review by Kim et al. (2016) the agroforestry systems increase N in soils, also application of manure (see Table 3.1) coupled with varied management practices leads to N gradient across the LUTs hence different $CH_4$ uptake levels. Low $CH_4$ uptake cumulatively and during SR 2020 season was observed. The explanation for this could be due to high soil organic carbon that function as substrates for methanogenesis processes. Also, animal trampling causes soil structure disturbances thus high soil bulk density, leading to the establishment of methanogenic archaea (Serrano-Silva et al., 2014).

The observed significant ($p$<0.0001) seasonal and LUT interactions could be attributed to the differences in crop performance and precipitation during the two cropping seasons. The low $CH_4$ uptakes during the L.R. 21 could be due to increased methane production. The applied manure not used by crops necessitated methane production, it could have also increase anaerobic microsites (Dutaur and Verchot, 2007), resulting in $CH_4$ production in different LUTs.

The cumulative annual soil $CO_2$ emissions ranged from 6509.86 to 14400.75 kg$CO_2$-C ha$^{-1}$, which was slightly higher compared to the previous studies in Kenya (Macharia et al., 2020; Wachiye et al.,2020; Musafiri et al., 2021) that found a range of 1391 to 6000 kg$CO_2$-

C $ha^{-1}$ emissions under similar conditions. Soil $CO_2$ emissions were seasonal and it followed major events such precipitation, ploughing, fertilization similar to observations by Pelster et al. (2017). There was a significant difference in $CO_2$ fluxes across LUTs and seasons, with grazing having high $CO_2$ emissions across the season. The highest soil $CO_2$ fluxes in grazing land could be attributed to high soil organic carbon available due to continuous root availability from *Solanum incanum* that could have favored nutrient pumping and consequently increased emissions. Additionally, the high amount of carbon concentration under grazing land (Table 3.2) could have provided the substrate and energy for microorganism thus high decomposition rates. Rosenstock et al. (2016) and Wachiye et al. (2021) found an increasing $CO_2$ emission with an increasing carbon in soils. this can explain the high $CO_2$ emissions under grazing land. Continuous availability of animal droppings for the entire study period explains high amounts of carbon compared to other LUTs. Also, $CO_2$ emissions can be elaborated by the positive correlation of SOC with the $CO_2$ emissions (see Table 3.5), therefore with an increase in carbon there is likelihood of increase in $CO_2$ emissions.

There were high $CO_2$ emissions under agroforestry systems (agroforestry L and agroforestry M) across the seasons, compared to the monocrops (Sole maize and sorghum) LUTs. These can be elaborated by availability of roots that increases carbon in soil compartment (Table 3.2) through root degradation. Additionally, the decomposition of leaf litter fall could increase the amounts of carbon thus high $CO_2$ emissions. On the contrary, the monocrops had low $CO_2$ emissions which could be due to low carbon in soils (Table 3.2). Generally, nutrient mining due to harvesting with limited nutrient replenishment could have resulted in low $CO_2$ emissions (Oartel et al., 2016). Also, high soil bulk density (Table 3.2) results to low soil atmosphere exchange due to low gas diffusivity hence low $CO_2$ fluxes.

The variability of $CO_2$ across the land utilization types can be attributed to the difference in vegetation; this immensely affects the rate of emissions as plants' roots. The photosynthesis rate differs, affecting respiration and photosynthesis, respectively (Oartel et al., 2016). The effect of textural characteristics in the LUTs could have majorly contributed to varied $CO_2$ emissions. Additionally, seasonal interactions reflect the effect of moisture on $CO_2$ (Wanyama et al., 2018b). However, this study only reported the soil $CO_2$ emissions (decomposition and root respiration). Therefore, the entire $CO_2$ budget from the soil and photosynthesis is essential.

The cumulative annual soil $N_2O$ fluxes across the land utilization types were consistent with previous studies in East Africa (Pelster et al., 2017; Ortiz-Gonzalo et al., 2017; Musafiri et al., 2020a). The amount of N fixed by Leucaena leucocephala under Agroforestry could have led to high $N_2O$ fluxes, which is could be explained by N as Leucaena leucocephala fixes atmospheric nitrogen to the soil (Cubillos-Hinojosa et al., 2019). The low soil $N_2O$ fluxes under the grazing land could be attributed to low nitrogen cycling due to low nitrogen content and low gas diffusivity that increases $N_2O$ consumption. The low $N_2O$ fluxes under sole sorghum could be explained by low SOC (Table 3.2) and removal of N through harvesting crops. In addition, there could have been low mineralization under sole sorghum and grazing land. Wanyama et al. (2018a) found low $N_2O$ emissions under similar conditions. The lowest soil $N_2O$ fluxes under grazing land could be attributed to the highest root production (Table 3.4), as indicated by the negative correlation of roots and $N_2O$ fluxes (Table 3.5). Low clay content contributed to low $N_2O$ fluxes, as indicated by the negative correlation with clay content (Table 3.5). additionally, low clay content necessitated nitrification process at the expense of denitrification. Low emissions $N_2O$ could also be due to the high gas diffusivity that increases the $N_2O$ consumption (Balaine et al., 2016) through limitation of the anaerobic microsites thus less denitrification process.

Crop residue retention is essential in improving fertility and yields (Kiboi et al., 2019). The novelty of crop residue retention on the field due to its ability to incorporate nutrients could have mixed effects on the soil N2O fluxes (Mutegi et al., 2010; Shan et al., 2013; Tongwane et al., 2016). Crop residue retention increased the induction of labile carbon that plays a fundamental role during the denitrification process by acting as electron donors (Butterbach-Bahl et al., 2013). The study was conducted on flood-prone soils that provided favorable conditions for $N_2O$ emissions. The crop residue retention could increase $N_2O$

fluxes. However, crop residue retention is limited in most Kenyan smallholder cropping practices due to livestock competition and fuel (Macharia et al., 2020; Musafiri et al., 2020b).

### 3.3.7 Maize and sorghum production

The grain yield ranged from 5221.5 kg $ha^{-1}$ (sole maize, n=3) to 505.3 kg $ha^{-1}$ (sole sorghum, n=3), Table 3.4). Low roots, leaves, and stems production were observed during the season (Table 3.4). The maize and sorghum crops planted by the smallholder farmer during the L.R. 21 failed due to poor rainfall timing. During the S.R. 20 seasons, the yield scaled $N_2O$ emissions ranged from 0.35 g $N_2O$-N $kg^{-1}$ grain yields under sole maize to 4.90 g $N_2O$-N $kg^{-1}$ grain yields under Agroforestry L. Yield scaled $N_2O$ emissions of 1.98 and 3.07 g $N_2O$-N $kg^{-1}$ grain yields were observed under sole sorghum and Agroforestry M.

**Table 3.4** Maize and sorghum production under different land utilization types during the S.R. 20 in Siaya County, Kenya

| LUTs[1] | Roots ($kgha^{-1}$) | Stems ($kgha^{-1}$) | Leaves ($kgha^{-1}$) | Grains ($kgha^{-1}$) | Total Biomass ($kgha^{-1}$) | N2O YSE (g N2O-N $kg^{-1}$) |
|---|---|---|---|---|---|---|
| Agroforestry M | 198.8 | 2446.5 | 1597.5 | 505.3 | 4748.1 | 3.07 |
| Sole Sorghum | 306.3 | 3258.0 | 2137.5 | 505.6 | 6207.4 | 1.98 |
| Agroforestry L | 141.4 | 1036.5 | 934.5 | 508.0 | 2620.4 | 4.90 |
| Sole maize | 203.0 | 3478.5 | 3942.0 | 5221.5 | 12845.0 | 0.35 |
| Grazing land[2] | - | - | - | - | - | - |

[1] LUTs is the land utilization types i) Agroforestry M (Agroforestry *Markhamia lutea* and sorghum), ii) sole sorghum (sorghum monocrop), iii) Agroforestry L (Sorghum and *Leucaena leucocephala)*, iv) sole maize (maize monocrop), and iv) grazing land.

[2] No crop planted in the grazing land

The sorghum grain yields (505 to 508 kg $ha^{-1}$ for one cropping season) were in corroboration with 464 to 540 reported by Njagi et al. (2019). However, the sorghum yields were lower than the potential sorghum productivity of 4000 kg $ha^{-1}$ (Muui et al., 2013). The maize grain yields of 5222 kg $ha^{-1}$ were consistent with those reported by previous studies in western Kenya, ranging between 500 to 5600 kg $ha^{-1}$ (*Güereña* et al., 2016; Ngome et al., 2013). The low sorghum productivity in the study area could be attributed to poor rain timing and agronomic management coupled with *Striga hermonthica* infestation. The *Striga hermonthica* is a significant threat to sorghum production in the study area resulting in reduced grain productivity (Midega et al., 2017). The calculated $N_2O$ yield scaled emissions that ranged between 0.35 to 4.90 g $N_2O$-N $kg^{-1}$ consistent with 0.024 to 67 g$N_2O$-N $kg^{-1}$ (Pelster et al., 2017; Macharia et al., 2020; Musafiri et al., 2020a). The low yield scaled emission could be attributed to the low soil greenhouse emissions across the land uutilization types. It is noteworthy that sole sorghum had higher yield-scaled $N_2O$ emissions than sole maize. This could be attributed to the low sorghum productivity due to poor management and *Striga hermonthica* infestation lowering the yields. Notably, the improved land utilization management such as agroforestry L and Agroforestry M led to increased yield-scaled $N_2O$ emissions. However, the yield scaled $N_2O$ emissions were based on cereal crop grain yields, and consider the agroforestry trees value.

### 3.3.8 Correlations between soil/ root data and soil GHG emissions

Soil $CO_2$ emissions were positively correlated to soil organic carbon ($p$=0.0001), soil moisture ($p$=0.04), and clay content ($p$=0.03), Table 3.4). The soil $N_2O$ fluxes were negatively correlated with soil bulk density ($p$=0.01), clay content ($p$=0.04), and roots ($p$=0.03), Table 3.4).

**Table 3.5** Correlations between soil/ root data and soil GHG emission

| **Parameter** | **$CH_4$ fluxes (kg $CH_4$-Cha$^{-1}$)** | **$CO_2$ emissions (kg$CO_2$-C ha$^{-1}$)** | **$N_2O$ fluxes (kg$N_2O$-Nha$^{-1}$)** |
|---|---|---|---|
| Soil bulk density (g $cm^{-3}$) | 0.08[1] | -0.08 | **-0.64**** |
| Soil organic carbon (%) | -0.23 | **0.83**** | -0.03 |
| Soil temperature (°C) | -0.23 | -0.48 | -0.21 |
| Soil moisture (g $g^{-1}$ of soil) | -0.25 | **0.52*** | 0.05 |
| Clay content (%) | -007 | **0.52*** | **-0.58*** |
| Roots (kg $ha^{-1}$) | -0.18 | -0.11 | **-0.62*** |

* = $p < 0.05$.
** = $p < 0.01$.
[1] = correlation coefficients (rho values).

### 3.4 Conclusions

There is a vast data gap on the quantity of soil GHG fluxes across different land utilization types in Kenya. Soil GHG fluxes were quantified from five common land utilization types that is i) Agroforestry M (Agroforestry *Markhamia lutea* and sorghum), ii) sole sorghum (sorghum monocrop), iii) Agroforestry L (Sorghum and *Leucaena leucocephala)*, iv) sole maize (maize monocrop) and iv) grazing land. In line with the hypothesis, soil GHG fluxes are significantly different across the land utilization types. There were seasonal and seasonal treatment interactions. There were highest soil $CO_2$ emissions, $CH_4$ uptake, and $N_2O$ fluxes under grazing land, sole maize, and agroforestry L. There were also lowest soil $CO_2$ emissions, $CH_4$ uptake, and $N_2O$ fluxes under sole maize, sole sorghum, and grazing land. The soil GHG fluxes were $CO_2$ emission, and the $CH_4$ uptake and $N_2O$ fluxes were of low magnitude though consistent with other studies in Kenya. The main drivers of soil GHG fluxes were soil bulk density, soil organic carbon, soil moisture, clay content, and root production. Following this finding, the is a need for future studies to consider the benefits of Agroforestry integration on the income among smallholder farmers that is income from crops, timber, and livestock feeding. This will give comprehensive trade-offs improved land utilization types (agroforestry) on smallholders' welfare expressed as income scaled $N_2O$ fluxes compared to monocropping. The findings are essential as they established the contribution of different smallholders' land utilization types, thus filling the data gap on the National GHG budget.

## CHAPTER FOUR

## MODELING NITROUS OXIDE FLUXES FROM DIFFERENT LAND UTILIZATION TYPES OF SIAYA COUNTY


### Abstract

The use of biogeochemical models such as the DeNitrification-DeComposition (DNDC) is vital during the simulation of GHG and understanding the interaction process between plants and soils. There is uncertainty on the capability of DNDC model to simulate plant soil and climate across land utilization types. There is a need to understand the GHG dynamics. The aim of the study was to simulate soil nitrous oxide fluxes under different land utilization types in Siaya county. The study used five land utilization types i) Agroforestry with *Markhamia luteau*, ii) sole sorghum, iii) Agroforestry with *Luecaeena leucocephala*, iv) sole maize and v) grazing land replicated thrice. The model was tested against the fields' moisture, soil temperature, and $N_2O$ fluxes from different land utilization types (LUTs). Soil $N_2O$ was sampled using static chambers. Nitrous oxide was analyzed using gas chromatography. The model showed a high degree of fit in simulating daily soil temperature, soil moisture, and soil $N_2O$ emissions. The model depicted good results during simulation of soil moisture; RMSE<5, 2% <nRMSE <15.54%, from 0.86< NSE <0.99, 0.03< $R^2$ <0.97 and d < 0.99. Daily soil temperature; 0.08 <RMSE< 1.33, from 0.3%< nRMSE< 5.9%, from 0.27< NSE< 0.99, from 0.12< $R^2$ <0.99. daily soil $N_2O$; 0.002 <RMSE< 0.006, 0.45% <nRMSE< 2.48%, NSE=0.99, from 0.5< $R^2$ <0.9, 0.98 <d< 0.99. The DNDC model showed relatively excellent results in simulating soil moisture, temperature, and $N_2O$ fluxes. The model perfectly fitted the $N_2O$ emissions peaks following the precipitations. The model can reliably be used to model $N_2O$ emissions and offers a cheaper approach to GHG emissions estimations.



**Keywords;** Land utilization types; Nitrous oxide; DNDC model; UNFCCC; Climate mitigation

### 4.1 Introduction

Agricultural lands contribute 14-17% of the GHG budget (Dangal et al., 2019). Land use and land-use change contribute to 50% of anthropogenic GHG emissions (He et al., 2011). Grazing land also contributes to up to 10% of the global emissions due to excreta deposition (Dangal et al., 2019). Increasing GHG concentration leads to the trapping of long wave radiation, thus increasing global warming (Lyon et al., 2020). Soil nitrous oxide is a potent GHG with a high radiative force of 265 (Pachauri et al., 2014). Agriculture contributes close to 60% of $N_2O$ emissions (Valentini et al., 2014; Tubiello, 2019) and plays a vital role in GHG budgets. Concerted efforts such as changing land utilization types and the use of inorganic fertilizers could exacerbate GHG emissions. The need for the production of more food could surge $N_2O$ emissions. Therefore, there is a need to carry out $N_2O$ estimations under different land utilization types (LUTs).

Nitrous oxide fluxes involve a complex biogeochemical process; decomposition of hydroxylamine, chemodenitrification, nitrification, and denitrification process (Butterbach-Bahl et al., 2013). Soil physicochemical properties such as bulk density, pH, organic carbon, and texture have influence on $N_2O$ fluxes (Abdalla et al., 2009; He et al., 2019). Soil moisture controls the availability of oxygen for soil microbes, thus denitrification or nitrification (Butterbach-Bahl et al., 2013). The change in land utilization types and management practices could lead to a change in soil climate. Denitrification is also very sensitive to temperature changes (Butterbach-Bahl et al., 2013), thus altering the $N_2O$ dynamics. Therefore, the need to simulate soil moisture and temperature.

Quantifying soil $N_2O$ fluxes from different land utilization types is key for an accurate and timely report to the United Nations Framework Convention on Climate Change (UNFCCC). Reporting of the GHG is based on IPCC Tier 1, where it is perceived that 0.9-1.25% of the applied N is released as oxides (Abdalla et al., 2011). Most countries use the Tier I emissions factors that have shown to overestimate the GHG emissions, reported by Macharia et al. (2020) and Musafiri et al. (2020) in Sub-Saharan Africa. Despite the need to estimate $N_2O$ emissions for policy implementation, field GHG quantification could mask variations and errors. Also, the expense used in maintaining flux measurement sites is high.

Simulation of GHG estimates soil $N_2O$ from agroecosystems by using climate and soil data. Modeling offers a great insight by linking the effects of soil climate on $N_2O$ fluxes. Modeling simulates the process such as nitrification and denitrification, which are the main processes for producing and consuming $N_2O$ over a long period, up to 100 years.

Online models have been devised for the simulation of $N_2O$ fluxes from agro-ecosystems. Models ranged from simple to complex, simulating all factors controlling $N_2O$ production and consumption (Li et al., 1992; Li et al., 1994). The DNDC model is widely used in simulating $N_2O$ fluxes from agroecosystems (Li, 2000). The rainfall model (Li et al., 1992) was also used in USA. The DNDC model has also been used in SSA to simulate $N_2O$ fluxes and crop performance (Macharia et al., 2021) and in different soil fertility management technologies (Musafiri et al., 2021). The DNDC has proven reliable in simulating the soil agricultural GHG in various setups such as cropland, grassland, and forestland. The DNDC contains four sub-models (Li, 2000); decomposition, denitrification, soil climate, and crop growth sub-models.

The objective of this study was to validate $N_2O$ fluxes of selected land utilization types in smallholder farms using DNDC model in Siaya County.

## 4.2 Material and methods

### 4.2.1 Site description

Greenhouse gas collection was done in selected smallholder land utilization types of Nyajuok sub-location, Siaya County, Western Kenya. The farm lies at 1236 m above sea level and is within the lower midland (LM1)- "sugarcane belt" agro-ecological zone. The area receives a biannual rainfall of 1500 mm and 1900 mm and an average temperature of 20.9 to 21.8 $^0$C. The dominant soil type in the study area is Ferralsols, with low fertility status, thus impels the soil nutrient amendment. The area is suitable for maize (*Zea mays*), sorghum (*Sorghum bicolar*), common beans (*Phaseolus vulgaris*), cowpeas (*Vigna unguiculata*), sweet potatoes (*Ipomoea batatas*), soya beans (*Glycine max*), sunflower (*Heliuthus annuus*), spinach (*Spinacia oleracea*), and onions (*Allium cepa*) (Jaetzold et al., 2010). The main LUTs are; agroforestry, grazing, sorghum, and maize (Jaetzold et al., 2010).

### 4.2.5 Nitrous oxide fluxes measurements and other field observations

Nitrous oxide was sampled following the static vented chamber technique. Three PVC chambers in every LUT were installed at the onset of the experiment. Briefly, chambers consisted of a lid (dimensions; 20cm by 8cm height and diameter) and a base (dimensions; 20 by 10cm height and diameter with 5cm below the ground). The pressure equilibrium is maintained by the existence of a vent and a rubber septum to ensure airtight sealing. Chambers were removed and reinstalled during major events such ploughing and planting. However, chambers in grazing land remain installed for the entire study period. Soil $N_2O$ was carried out bi-weekly and during major activities such ploughing, fertilization, weeding and rainfall events (Parkin and Venterea 2010; Macharia et al., 2020). The sampling campaigns were carried out between 0800hrs and 1200hrs. Soil $N_2O$ sampling was carried out at intervals of 0-, 10-, 20-, and 30-min using a 60 ml syringe fitted with a Luer lock. The gas samples were then taken to Mazingira Centre (ILRI-- Nairobi, Kenya) for analysis of $N_2O$ using SRI 8610C gas chromatography (2.74m Hayesep-D column) fitted with a $^{63}$Ni-electron capture detector (ECD) for $N_2O$.

Gas Chromatography (GC) was calibrated after every four samples, where the fifth sample analyzed on the gas chromatograph was the calibration gas**.** The soil GHG fluxes were calculated by accounting for environmental factors, including air pressure and temperature, following the ideal gas law (Pelster et al., 2017; Macharia et al., 2020; Musafiri et al., 2020). The cumulative seasonal and annual fluxes with calculated by linear interpolation between sampling events following the trapezoidal rule.

Plant biomass data were collected during the same period the soil $N_2O$ from the planting to the harvesting time. Other data collected during the study period are; soil moisture and soil temperature using a thermometer (TFA thermometer, Zum Ottersberg, Wertheim, Germany). Additionally, the climate data were collected using HOBO U30 NRC station data logger installed at the study site.

### 4.2.2. The DNDC Model

DNDC model version 9.5 was downloaded to model soil temperature, moisture and $N_2O$ fluxes from different smallholders' land-utilization types. DeNitrification DeComposition model is a simulator of C and N biogeochemistry in agroecosystems. The model framework includes the environmental, C, and N dynamics and the edaphic and trace gas fluxes which are reported daily (Jarecki et al., 2018; Macharia et al., 2021). The DNDC Model was initially used to predict C and GHG emissions (Li et al., 1992). DeNitrification DeComposition model consists of the following components: soil-climate, crop growth, and decomposition sub-models which predict soil temperature, soil pH, and soil moisture and substrate concentration that is based mainly on the anthropogenic activities as the ecological driver. The first sub-model for soil (SOC, texture, and the hydraulic factors, climate (wind speed, humidity, precipitation, temperature, solar radiation, crop factors (crop type, water demand, potential yield, C/N ratio), management practices (tillage, planting time, irrigation, fertilizer, harvest date) and decomposition (labile humus, microbial biomass, and passive humus). The model converts; climate, soil, human activities, and vegetation into soil environmental factors; Ph, redox potential, humidity, soil temperature, and difference in concentration of substrates. The second one includes nitrification, denitrification, and fermentation sub-models, which predict C and N gas flux, such as $N_2O$ and $CH_4$ (Li, 2000). Evaluation of the DNDC model for the six sub-models is derived from the biological, chemical, and physical theories between the model and measured or the field data.

### 4.2.3 The DNDC model parametrization

To model the trace gas emissions ($N_2O$), The HOBO U30 NRC station data logger installed at the study site was used to collect; maximum and minimum temperature (0C), precipitation (mm), solar radiation (M J $m^{-2}$ $day^{-1,}$ and relative humidity (%). The file was prepared following the DNDC guide. Soil sampling was done for laboratory analysis. The samples were used to test for the soil organic carbon, bulk density, pH, Field capacity and texture (Table 4.1 and 4.2). Soil characteristics such as wilting point, soil porosity, conductivity, and field capacity were obtained from the Soil - Plant - Atmosphere - Water Field & Pond Hydrology (S-P-A-W model) (Parry, R) Collection of data on the site management and crop data such as; tillage method, land preparation date, type of crop, planting date, biomass C/N ratio, fertilizer data (method of fertilization, amount of fertilizer applied, fertilization date, and manure application (type of manure, date of application, method of application was done. The data on grazing (grazing intensity, type of animals grazing on the field) was collected throughout the study period.

**Table 4.1** Model input parameters used in modeling of soil $N_2O$ fluxes from different land utilization types of Siaya County.

| **Parameter** | **Value/ Unit** |
|---|---|
| ***Climate*** | |
| Annual precipitation | 15711mmyear$^{-1}$ |
| Maximum temperature | 26.77 $^0$Cday$^{-1}$ |
| Minimum temperature | 19.00 $^0$Cday$^{-1}$ |
| Wind speed | 1.88 ms$^{-1}$ |
| Solar radiation | 11.41 MJm$^{-2}$day$^{-1}$ |
| Humidity | 71.42 %Day$^{-1}$ |
| ***Soil properties*** | |
| Soil bulk density | Measured gcm$^{-3}$ |
| Soil organic carbon | Measured kgC/kg of soil |
| Clay fraction | Measured % |
| Wilting point | Measured |
| Field capacity | Measured |
| Hydraulic conductivity | Measured |
| C/N ratio | Default values |
| SOC partitioning | Defaults values |

**Table 4.2** Baseline soil properties under different land utilization types at 0-20 cm depth in Siaya County, Kenya

| **LUTs[1]** | **Bulk density (g cm$^{-1}$), n=3)** | **Soil organic carbon (%), n=3)** | **Soil pH (n=1)** | **Soil texture (%), n=1)** | | |
|---|---|---|---|---|---|---|
| | | | | Sand | Clay | Silt |
| Agroforestry M | 1.23$^c$ | 2.23$^a$ | 5.2 | 47 | 19 | 34 |
| Sole sorghum | 1.40$^b$ | 1.50$^b$ | 4.9 | 48 | 15 | 37 |
| Agroforestry L | 1.20$^c$ | 2.07$^a$ | 5.4 | 46 | 18 | 36 |
| Sole maize | 1.50$^a$ | 0.61$^c$ | 4.8 | 52 | 18 | 30 |
| Grazing land | 1.53$^a$ | 2.01$^a$ | 5.1 | 50 | 18 | 32 |
| *P* value | <0.0001 | <0.0001 | | - | - | - |

[1] LUTs is the land utilization types i) Agroforestry M (Agroforestry *Markhamia lutea* and sorghum*)*, ii) sole sorghum (sorghum monocrop), iii) Agroforestry L (Sorghum and *Leucaena leucocephala)*, iv) sole maize (maize monocrop), and iv) grazing land.
[2] Mean bulk density and soil organic carbon with the same superscript in the same column during the season are not significantly different between land utilization types at $p \leq 0.05$.

### 4.2.4 Model calibration and accuracy determination

The DNDC model was calibrated to predict $N_2O$ using field data from different LUTs

(Table 4.1 and 4.2). The field data was input and the default data and consequently optimize by using soil properties such as soil organic carbon, soil bulk density, soil pH, and C/N ratio, crop parameters i.e the biomass ratios, the total biomass, roots, leaves, stems and grains. The grain yield was converted into carbon equivalent following the DNDC guide, where the field data was multiplied by 0.4 (Li, 2012; Musafiri et al., 2021). The DNDC model was then run across the different LUTs using the optimized input parameters.

The DNDC model goodness of fit was evaluated during modeling of $N_2O$ fluxes, soil temperature, soil moisture from different land utilization types using the following matrices; mean error (ME), root mean square error (RMSE), and normalized root mean square error (NRMSE), Nash-Sutcliffe efficiency (NSE) and willmont index of agreement (d).

$$\mathrm{ME} = \frac{\Sigma \mathrm{i}(\mathrm{Si}-\mathrm{Mi})}{\mathrm{n}} \tag{4.1}$$

$$\mathrm{RMSE} = \sqrt{\frac{\sum_{\mathrm{i}=1}^{\mathrm{n}}(\mathrm{Si}-\mathrm{Mi})^2}{\mathrm{n}}} \tag{4.2}$$

$$\mathrm{NRMSE} = \frac{\sqrt{\sum_{\mathrm{i}=1}^{\mathrm{n}}(\mathrm{Si}-\mathrm{Mi})^2/\mathrm{n}}}{\mathrm{M}} \times 100 \tag{4.3}$$

$$\mathrm{NSE} = 1 - \frac{\sum_{\mathrm{i}=1}^{\mathrm{n}}(\mathrm{Si}-\mathrm{Mi})^2}{\sum_{\mathrm{i}=1}^{\mathrm{n}}(\mathrm{Mi}-\dot{\mathrm{M}})^2} \tag{4.4}$$

$$d = 1 - \frac{\sum_{i=1}^{n}(Si-Mi)^2}{\sum_{i=1}^{n}(|\mathrm{Si}-\mathrm{M}|+|\mathrm{Mi}-\mathrm{M}|)^2} \tag{4.5}$$

Where $S_i$ is the simulated value, $M_i$ is the measured value, n is the number of measurements, $\dot{M}$ is the average of the observed values.

The DNDC The NRMSE (%) statistic can be used to compare simulation performance between datasets or models with different scales. The model was considered excellent when the nRMSE<10% We considered an ‘‘excellent” model performance when the NRMSE<10%, ‘‘good” performance when 10% < NRMSE depicted a good fit between the model and the field when NSE ≥0.5 (Musafiri et al., 2021). The model was considered fit when the $R^2$ >0.5. The NSE (0 to 1) is a normalized measure that determines a relative magnitude of model residuals compared to the measured variance, a NSE value between 0.0 and 1.0 is generally viewed as acceptable model performance (He et al., 2019). The d

(0 to 1) has no dimensions with values approaching 1 indicating better agreement. The model was also considered excellent based on the value agreement (d), where $d<0.7$ is poor, $0.8<d<0.9$ is fair, while $d>0.9$ shows a good fit (Jiang et al., 2021). The field $N_2O$ fluxes was subjected to ANOVA using SAS 9.4 and the mean difference between LUTs separated using Tukey's honest significance difference (HSD) test at $p<0.05$.

### 4.2.5 Yield-scaled $N_2O$ emissions

Yield-scaled emissions $N_2O$ was calculated by dividing soil $N_2O$ fluxes with annual grain yields following equation 4.6

$$\mathrm{YSE} = \frac{\text{Annual N2O fluxes}}{\text{Grain yield}} \qquad (4.6)$$

## 4.3 Results and Discussion

### 4.3.1 Soil temperature, moisture and Yield scaled emission

The DNDC model showed accurate results from the estimation of soil temperature. The model temperatures predicted the actual temperatures from the field except under sole Sorghum. The ME from -2.04 to -1.9$^0$C. RMSE from 0.08 to 1.33 $^0$C, nRMSE from 0.3 to 5.9 %, NSE from 0.27 to 0.99, $R^2$ from 0.12 to 0.99 and d>0.9 for all the LUTs (Table 4.3), which shows that the model accurately predicted the soil temperature across all the LUTS except under sole sorghum. The findings agreed with Li et al. (2017), who found high model soil temperature compared to the field temperature. The results were against that of Uzoma et al. (2015), who found an underestimation of soil temperature. The estimation of temperature is vital as it influences the GHG fluxes. Temperature influences microbial activities and soil moisture, thus influencing GHG emissions. Therefore, proper soil temperature estimation is vital due to its direct influence on the GHG fluxes. High estimation of temperatures could partly be linked to the low soil fertility, thus limiting the growth of crops hence increasing the thermal radiation. The grazing land, however, could be due to the unavailability of the canopy cover thus high thermal radiation in soil compartments.

**Table 4.3** Statistical model evaluation of soil moisture and temperature of different land utilization types of Siaya County

| LUT | Model | Field | ME | RMSE | nRMSE | NSE | $R^2$ | d |
|---|---|---|---|---|---|---|---|---|
| ***Soil temperature (°C)*** | | | | | | | | |
| Agroforestry M | 24.87 | 24.55 | -2.04 | 1.33 | 5.43 | 0.68 | 0.99 | 0.99 |
| Sole Sorghum | 24.89 | 24.61 | -2.04 | 0.083 | 0.34 | 0.99 | 0.12 | 0.99 |
| Agroforestry L | 24.87 | 22.45 | -1.90 | 1.33 | 5.9 | 0.27 | 0.99 | 0.99 |
| Sole Maize | 24.83 | 25.93 | -2.16 | 1.33 | 5.13 | 0.86 | 0.98 | 0.99 |
| Grazing land | 24.89 | 23.37 | -1.94 | 1.33 | 5.69 | 0.51 | 0.99 | 0.99 |
| ***Soil moisture (%)*** | | | | | | | | |
| Agroforestry M | 0.26 | 0.21 | -0.02 | 0.02 | 7.04 | 0.96 | 0.89 | 0.99 |
| Sole Sorghum | 0.23 | 0.22 | -0.02 | 0.01 | 2.10 | 0.99 | 0.033 | 0.99 |
| Agroforestry L | 0.24 | 0.22 | -0.02 | 0.01 | 6.66 | 0.96 | 0.87 | 0.99 |
| Sole Maize | 0.37 | 0.16 | -0.01 | 0.02 | 15.54 | 0.86 | 0.97 | 0.99 |
| Grazing land | 0.16 | 0.19 | -0.01 | 0.02 | 8.35 | 0.94 | 0.84 | 0.99 |

LUT[1] Agroforestry M= Agroforestry with *Markhamia lutea*, Agroforestry L= Agroforestry with *Leucaena leucocephala*

Soil moisture is primarily a function of precipitation. The DNDC model accurately simulated the soil moisture content across different LUTs. Soil moisture simulation was overestimated across the LUTs except for the grazing Land that showed underestimation. The ME ranges from -0.2 to -0.1 g $g^{-1}$, RMSE from 0.01 to 0.2, nRMSE from 2 to 15.54%, NSE from 0.86 to 0.99, $R^2$ from 0.03 to 0.97 and d was the same (0.99) across the LUTs (Table 4.3). The soil moisture was perfectly estimated across all the LUTs despite the area recording a lower amount of precipitation (Table 4.1) compared to the seasonal average reported by Jaetzold et el. (2010). The results agreed with the findings of Uzoma et al. (2015) and Macharia et al. (2021), who reported an overestimation despite the low average precipitation of 9-15%. Further, these results were similar to those of He et al. (2019), who found a high estimation of soil moisture content by the DNDC at the 0-10cm depth. The ability of DNDC to predict soil water flow in the hydrological sub-models could have led to the perfect estimation of soil moisture content (Dutta et al., 2016). Soil moisture directly influences the soil GHG emissions; thus, overestimation could directly lead to overestimation of the GHG ($N_2O$) emissions. The model showed a conflicting result to that of Smith et al. (2008), who found an underestimation of soil moisture content. It is worth noting that the addition of leaf litter fall under the agroforestry treatments (Agroforestry M and Agroforestry L) could have increased water retention due to increased soil organic matter (SOM), thus high storage of moisture in soils.

The DNDC model exhibited low YSE compared to the observed YSE across the LUTs (Table 4.4). Additionally, the DNDC model underestimated the crop productivity in the study area.

**Table 4.4** Maize and sorghum performance under different land utilization types of Siaya County

| LUTs[1] | | Sorghum parameters (kg $ha^{-1}$) | | | | | YSE (g $N_2O$-N $kg^{-1}$) |
|---|---|---|---|---|---|---|---|
| | | **Leaf** | **Stem** | **Roots** | **Grains** | **Total Biomass** | |
| Agroforestry M | Simulated | 138 | 218 | 295 | 782 | 1431 | 1.17 |
| | Observed | 198.8 | 2446 | 1597 | 505 | 4748 | 3.07 |
| Sole sorghum | Simulated | 146 | 129 | 222 | 644 | 1140 | 0.92 |
| | Observed | 306.3 | 3258 | 2137 | 505 | 6207 | 1.98 |
| Agroforestry L | Simulated | 86.0 | 111 | 152 | 563 | 912 | 2.7 |
| | Observed | 141.4 | 1036 | 934 | 508 | 2620 | 4.90 |
| Sole maize | Simulated | 235.5 | 247 | 309 | 5989 | 6780 | 0.2 |
| | Observed | 203.0 | 3478 | 3942 | 5221.5 | 12845.0 | 0.35 |
| Grazing land[2] | - | - | - | - | - | - | - |

[1] LUTs is the land utilization types i) Agroforestry M (Agroforestry *Markhamia lutea* and sorghum), ii) sole sorghum (sorghum monocrop), iii) Agroforestry L (Sorghum and *Leucaena leucocephala)*, iv) sole maize (maize monocrop), and iv) grazing land.
[2] No crop planted in the grazing land

The DNDC model underestimated crop performance (Table 4.4). The underestimation of the area's crop performance could be ascribed to low nutrient amendment and uneven rainfall distribution during SR 20. Results from this study corroborate with that of Zhang et al. (2018). Contrary to the results of this study, Muhammed et al. (2018); found an overestimation of crop yields.

### 4.3.3 Modeling of $N_2O$ fluxes

The daily modeled $N_2O$ fluxes ranged from 0.0 to 49 g $N_2O$-N $ha^{-1}$ $day^{-1}$ (Figure 4.1), while the field $N_2O$ fluxes ranged from 0.75 to 2.05 g $N_2O$-N $ha^{-1}$ $day^{-1}$. Generally, the model $N_2O$ fluxes were in agreement with the field $N_2O$ fluxes where ME ranged from -0.06 to -0.02 g $N_2O$-N $ha^{-1}$ $day^{-1}$, RMSE ranged from 0.002 to 0.006 g $N_2O$-N $ha^{-1}$ $day^{-1}$, nRMSE from 0.45% to 2.48%, NSE remained the same across the LUTs, $R^2$ from 0.5 to 0.9, d-statistic from 0.98 to 0.99 (Table 4.5). The model depicted a good fit based on the NSE>0.5 and the nRMSE<10%. The model $N_2O$ fluxes showed a substantial agreement with the field $N_2O$ fluxes. The model, however, predicted low $N_2O$ fluxes across most of the study period. The DNDC model predicted high $N_2O$ fluxes at the onset of the precipitation due to soil rewetting and most cases, coincided with fertilization in all the LUTs except grazing land.

**Table 4.5** Daily modeled and observed nitrous oxide (g $N_2O$-N $ha^{-1}$ $day^{-1}$) fluxes from different land utilization types of Siaya County

| LUT | Field | simulated | ME | RMSE | nRMSE | NSE | $R^2$ | d |
|---|---|---|---|---|---|---|---|---|
| Agroforestry M | $1.75^{a}\pm0.15$ | 1.67 | -0.04 | 0.004 | 0.77 | 0.99 | 0.7 | 0.99 |
| Sole Sorghum | $0.97^{b}\pm0.05$ | 1.00 | -0.04 | 0.006 | 1.26 | 0.99 | 0.9 | 0.99 |
| Agroforestry L | $2.55^{a}\pm0.02$ | 2.45 | -0.06 | 0.003 | 0.51 | 0.99 | 0.6 | 0.98 |
| Sole Maize | $0.56^{b}\pm0.14$ | 0.50 | -0.05 | 0.002 | 0.45 | 0.99 | 0.5 | 0.99 |
| Grazing land | $0.83^{b}\pm0.19$ | 0.73 | -0.02 | 0.0063 | 2.48 | 0.99 | 0.66 | 0.97 |
| *P*-value | 0.0001 | | | | | | | |

LUT[1] Agroforestry M= Agroforestry with *Markhamia lutea*, Agroforestry L= Agroforestry with *Leucaena leucocephala*

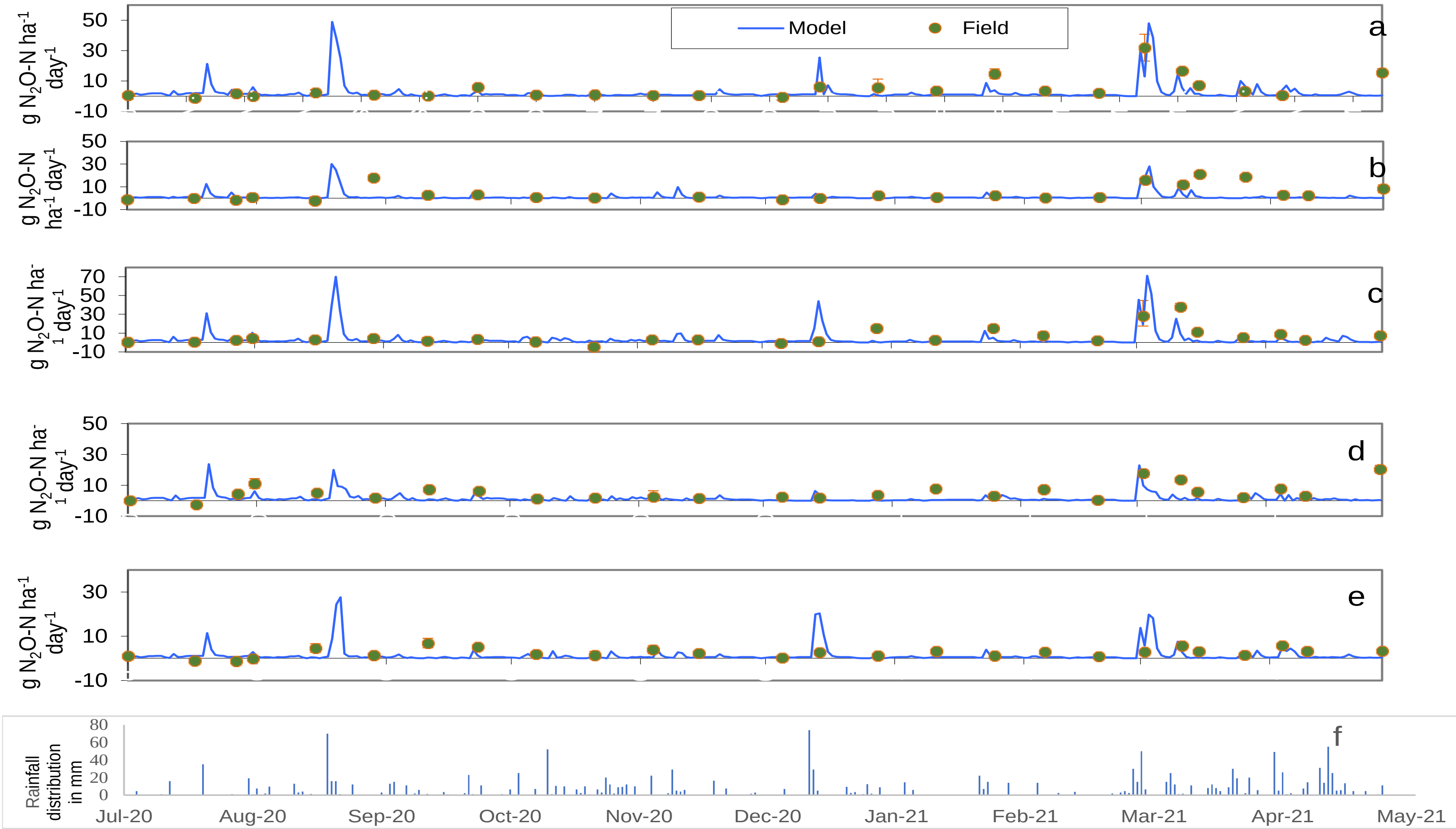


**Figure 4.1** Comparison between model and Field $N_2O$ fluxes (g $N_2O$-N $ha^{-1}$ $day^{-1}$) from different LUTs; (a) Agroforestry with *Markhmia lutea* (b) Sole sorghum (c) Agroforestry with *Leucaena leucocephla* (d) sole maize (e) Grazing Land of Siaya County and (f) precipitation

The DNDC exhibited an underestimation of daily $N_2O$ fluxes on most days of the study period, which was consistent with the findings of Macharia et al. (2021). The model showed peaks in $N_2O$ fluxes at the onset of precipitation and during fertilization. However, there were instances when DNDC underestimated the daily $N_2O$ fluxes despite the availability of rains. The $N_2O$ fluxes underestimation could be attributed to the high percentage of sand and silt fraction across the LUTs, which influence the soil hydrology sub-models. The DNDC could thus underestimate the $N_2O$ fluxes due to underestimating the denitrification process that yields the $N_2O$. Additionally, the $N_2O$ fluxes underestimation could be due to soil draining, influencing the soil moisture status (Smith et al., 2008). Even though soil moisture is a function of precipitation, the draining of soil water could have led to the un-simulation of the lateral flow of soil water (Uzoma et al., 2015).

The high amounts of modeled $N_2O$ fluxes under agroforestry L and agroforestry M could be attributed to high substrates inform of Dissolve Organic Carbon (DOC) from the SOM that has been buildup from leaf litterfall and root degradation. The DOC provided energy for the denitrifying bacteria (Xiang et al., 2022). According to Li et al. (2010), the availability of labile carbon that are substrates for the $N_2O$ emissions through denitrification and nitrification processes. Therefore, agroforestry treatments (Agroforestry M and Agroforestry L) improve the buildup of SOM and consequently SOC, which conserves soil moisture, thus leading to the production of $N_2O$ through denitrification.

The modeled and field $N_2O$ fluxes peak coincided with the precipitation and fertilization events. Giltrap et al. 2010,) Abdalla et al. (2020), and Musafiri et al. (2021) found similar results to the findings of this study. The DNDC model failed to simulate daily $N_2O$ uptake across the LUTs, identical to Rafigue et al. (2011) and Musafiri et al. (2021) reported $N_2O$ sink, which the DNDC model unpredicted. The $N_2O$ consumption is directly linked to $N_2O$ reduction to $N_2$ in the denitrification process (Butterbach- Bahl et al., 2013). The instances of $N_2O$ sink could be attributed to low gas diffusivity that favors $N_2O$ consumption at the expense of $N_2O$ production (Lide et al., 2010; Balaine et al., 2016), thus favoring the growth of nitrifying bacteria.

### 4.4 Conclusion

The applicability of DNDC depends on the precipitation, changes in farm inputs, and the general change in land utilization types. The DNDC model perfectly estimated soil temperature and soil moisture across all the LUTs grazing land, where soil moisture was underestimated. The DNDC model showed a high index of agreement (d>0.8) during the modeling of soil moisture, soil temperature, and $N_2O$ fluxes. The model predicted the effects of precipitation on $N_2O$ fluxes. However, daily $N_2O$ fluxes were underestimated in most parts of the study period. It is worthy to note that the average daily $N_2O$ fluxes were slightly lower than the modeled data. The DNDC model evaluation exhibited a good fit; hence, the model is reliable in simulating soil moisture, temperature, and $N_2O$ fluxes. Thus, the model can be an alternative approach for estimating trace gas emissions from agroecosystems, thus improving the accuracy of data reporting to UNFCCC. Therefore, the DNDC model can be used to fill a dearth in data availability and reporting for policy-making among climate adaptation and mitigation practitioners.

# CHAPTER FIVE

# SYNTHESIS, CONCLUSIONS, AND RECOMMENDATIONS

## 5.1 Synthesis

The study's main aimed was to quantify soil carbon stocks and greenhouse gas fluxes in selected smallholders' land utilization types in Siaya County, Kenya. This was addressed by quantifying SOC stock (Chapter 2), quantifying $CO_2$, $CH_4$, and $N_2O$ (Chapter 3), and modeling $N_2O$ fluxes (chapter 4). The main focus of chapter four was to test the applicability of the DNDC model in simulating agricultural trace gas emissions from different land utilization types of Siaya County.

Soil organic carbon is linked to soil texture and organic matter, a direct function of SOC, soil bulk density, and change across land utilization types (chapter 2). Changing Land utilization types have a strong effect on soil bulk density. Tillage and grazing directly impacted SOC concentrations and, consequently, SOC stock. This research offers avenues to improve SOC inputs in soils, thus soil productivity, such as practicing agroforestry systems. Thus, increase in climate adaptation among the smallholder farmers.

The drivers of GHG fluxes were soil bulk density, soil moisture which is a function of precipitation, roots availability, and animal droppings. Change in land utilization types changes the soil climate leading to the production of agricultural trace gas emissions. Different soil conditions yield different gases; an increase in soil bulk density increases the development of methanogenic archaea that necessitate the production of $CH_4$. An increase in soil moisture coupled with farm amendments leads to the production of $N_2O$ and $CO_2$. Generally, the change in land utilization types has an adverse effect on soil GHG emissions (chapter 3). Thus, the information can be used to improve the accuracy of reporting GHG in-situ measurements to UNFCCC and by climate change-related policymakers while designing and implementing climate change adaptation and mitigation strategies.

The biogeochemical model-simulated soil $N_2O$ fluxes from different land utilization types (chapter 4) offers an alternative method for measuring GHG fluxes. It also reduces GHG uncertainty and improves understanding of GHG dynamics. The DNDC model accurately simulated soil $N_2O$ fluxes from the LUTs in Siaya county. Therefore, offering a cheap and accurate estimation of agricultural trace gas emissions.

## 5.2 Conclusions

Based on the study's findings, the following conclusions were made:

1. Land utilization types of Siaya County influence SOC stock storage.
2. Land utilization types of Siaya County influence GHG fluxes, and the main drivers were SOC and soil bulk density.
3. The DNDC model showed a good fit in simulating soil GHG fluxes across land utilization types of Siaya County.

## 5.3 Recommendations

Based on the study, the following recommendations are drawn:

1. Practising improved LUT such as Agroforestry with *Leucaena sp* and Agroforestry with *Markhamia sp* improves SOC stock storage.
2. Quantifying soil GHG fluxes across LUTs aids in updating data inventories and reporting to UNFCCC.
3. The use of the DNDC model in simulating soil GHG provides site-specific GHG estimates.

## 5.4 Further study

The following areas need further research:

1. Further research is required to study the sequestration potential of different land utilization types in Siaya County
2. There is a need to include other LUTs during GHG quantification and the use of DNDC to improve the accuracy.

## REFERENCES


Abdalla, M., Song, X., Ju, X., Topp, C. F., & Smith, P. (2020). Calibration and validation of the DNDC model to estimate nitrous oxide emissions and crop productivity for a summer maize-winter wheat double cropping system in Hebei, China. *Environmental Pollution*, *262*, 114199.

Abdalla, M., Wattenbach, M., Smith, P., Ambus, P., Jones, M., & Williams, M. (2009). Application of the DNDC model to predict emissions of $N_2O$ from Irish agriculture. *Geoderma*, *151*(3-4), 327-337.

Abegaz, A., Tamene, L., Abera, W., Yaekob, T., Hailu, H., Nyawira, S.S., Da Silva, M.& Sommer, R. (2020). Soil organic carbon dynamics along chrono-sequence land-use systems in the highlands of Ethiopia. Agriculture, *Ecosystems & Environment*, 300, 106997.

Alemán-Ramirez, J. L., Okoye, P. U., Torres-Arellano, S., Mejía-Lopez, M., & Sebastian, P. J. (2022). A review on bioenergetic applications of Leucaena leucocephala. *Ind Crops Prod*, *182*, 114847.

Anokye, J., Logah, V., & Opoku, A. (2021). Soil carbon stock and emission: estimates from three land-use systems in Ghana. *Ecological Processes*, *10*(1), 1-13.

Ares, A., Neill, A. R., & Puettmann, K. J. (2010). Understory abundance, species diversity and functional attribute response to thinning in coniferous stands. *Forest Ecology and Management*, *260*(7), 1104-1113.

Balaine, N., Clough, T. J., Beare, M. H., Thomas, S. M., & Meenken, E. D. (2016, May). Soil gas diffusivity controls $N_2O$ and $N_2$ emissions and their ratio. *Soil Sci Soc Am*.

Barton, L., Wolf, B., Rowlings, D., Scheer, C., Kiese, R., Grace, P., Stefanova, K.& Butterbach-Bahl, K. (2015). Sampling frequency affects estimates of annual nitrous oxide fluxes. Scientific reports, 5(1), 1-9.

Bédard, C., Knowles, R., (1989). Physiology, biochemistry, and specific inhibitors of $CH_4$, $NH_4^+$, and CO oxidation by methanotrophs and nitrifiers. *Microbiol Rev*, 53, 68-84.

Bikila, N. G., Tessema, Z. K., & Abule, E. G. (2016). Carbon sequestration potentials of semi-arid rangelands under traditional management practices in Borana, Southern Ethiopia. Agriculture, *Ecosystems & Environment*, 223, 108-114.

Birch-Thomsen, T., Elberling, B., Fog, B., & Magid, J. (2007). Temporal and spatial trends in soil organic carbon stocks following maize cultivation in semi-arid Tanzania, East Africa. *Nutrient Cycling in Agroecosystems*, 79(3), 291-302.

Blanco-Canqui, H., Stone, L. R., Schlegel, A. J., Lyon, D. J., Vigil, M. M. Mikha, P. W. Stahlman, and C. W. (2009). No-till induced increase in organic carbon reduces maximum bulk density of soils. *Soil Science Society of America Journal*, 73(6), 1871-

1879.

Bolinder, M. A., Crotty, F., Elsen, A., Frac, M., Kismányoky, T., Lipiec, J., ... & Kätterer, T. (2020). The effect of crop residues, cover crops, manures and nitrogen fertilization on soil organic carbon changes in agroecosystems: a synthesis of reviews. *Mitigation and Adaptation Strategies for Global Change*, *25*(6), 929-952.

Bond-Lamberty, B., Wang, C., & Gower, S. T. (2004). A global relationship between the heterotrophic and autotrophic components of soil respiration?. Global Change Biology, 10(10), 1756-1766.

Brakas, S. G., & Aune, J. B. (2011). Biomass and carbon accumulation in land use systems of Claveria, the Philippines. In Carbon sequestration potential of Agroforestry systems (pp. 163-175). *Springer, Dordrecht*.

Bruun, T. B., Elberling, B., de Neergaard, A., & Magid, J. (2015). Organic carbon dynamics in different soil types after conversion of forest to agriculture. Land Degradation & Development, 26(3), 272-283.

Butterbach-Bahl, K., Baggs, E. M., Dannenmann, M., Kiese, R., & Zechmeister-Boltenstern, S. (2013). Nitrous oxide emissions from soils: how well do we understand the processes and their controls?. *Philosophical Transactions of the Royal Society B: Biological Sciences*, *368*(1621), 20130122.

Cardinael, R., Chevallier, T., Barthès, B. G., Saby, N. P Parent, T., Dupraz, C., Bernoux, M. and Chenu, C. (2015). Impact of alley cropping agroforestry on stocks, forms and spatial distribution of soil organic carbon—A case study in a Mediterranean context. *Geoderma*, 259, 288-299.

Cavanagh, C. J., Chemarum, A. K., Vedeld, P. O., & Petursson, J. G. (2017). Old wine, new bottles? Investigating the differential adoption of 'climate-smart'agricultural practices in western Kenya. *Journal of rural studies*, 56, 114-123.

Chaudhari, P. R., Ahire, D. V., Ahire, V. D., Chkravarty, M., & Maity, S. (2013). Soil bulk density as related to soil texture, organic matter content and available total nutrients of Coimbatore soil. *International Journal of Scientific and Research Publications*, 3(2), 1-8.

Chi, J., Waldo, S., Pressley, S., O'Keeffe, P., Huggins, D., Stöckle, C., Pan, W.L., Brooks, E., Lamb, B., (2016). Assessing carbon and water dynamics of no-till and conventional tillage cropping systems in the inland Pacific Northwest US using the eddy covariance method. *Agric. For. Meteorol*. 218, 37-49.

County, S. (2018). County Integrated Development Plan (CIDP). *Siaya County, 2022*.

Cubillos-Hinojosa, J. G., Milian-Mindiola, P. E., Hernández-Mulford, J. L., & Peralta-Castilla, A. (2019). Biological fixation of nitrogen by native isolates of Rhizobium sp. symbionts of Leucaena leucocephala (Lam.) De Wit. Acta Agronómica, 68(2), 75-

83.

Dangal, S. R., Tian, H., Xu, R., Chang, J., Canadell, J.G., Ciais, P., Pan, S., Yang, J. and Zhang, B. (2019). Global nitrous oxide emissions from pasturelands and rangelands: magnitude, spatiotemporal patterns, and attribution. *Global Biogeochemical Cycles*, *33*(2), 200-222.

De Groote H, Vanlauwe B,,Rutto E,, Odhiambo G.D,,Kanampiu F, & Khan Z.R., (2010). Economic analysis of different options in intergrated pest and soil fertility management in maize systems of Western Kenya. *Agricultural Economics* 41,471-482.

Degu, M., Melese, A., & Tena, W. (2019). Effects of soil conservation practice and crop rotation on selected soil physicochemical properties: The case of Dembecha district, Northwestern Ethiopia. *Applied and Environmental Soil Science*, 2019.

Deng, Q., Hui, D., Wang, J., Yu, C. L., Li, C., Reddy, K. C., & Dennis, S. (2016). Assessing the impacts of tillage and fertilization management on nitrous oxide emissions in a cornfield using the DNDC model. *Journal of Geophysical Research: Biogeosciences*, *121*(2), 337-349.

Dutaur, L., & Verchot, L. V. (2007). A global inventory of the soil CH4 sink. Global biogeochemical cycles, 21(4).

Dutta, B., Smith, W. N., Grant, B. B., Pattey, E., Desjardins, R. L., & Li, C. (2016). Model development in DNDC for the prediction of evapotranspiration and water use in temperate field cropping systems. *Environmental Modelling & Software*, *80*, 9-25.

Eid, E. M., Khedher, K. M., Ayed, H., Arshad, M., Moatamed, A., & Mouldi, A. (2020). Evaluation of carbon stock in the sediment of two mangrove species, Avicennia marina and Rhizophora mucronata, growing in the Farasan Islands, Saudi Arabia. *Oceanologia*, 62(2), 200-213.

Gao, Y., Zhou, J., Wang, L., Guo, J., Feng, J., Wu, H., & Lin, G. (2019). Distribution patterns and controlling factors for the soil organic carbon in four mangrove forests of China. *Global Ecology and Conservation*, *17*, e00575.

Giltrap, D. L., Li, C., & Saggar, S. (2010). DNDC: A process-based model of greenhouse gas fluxes from agricultural soils. *Agriculture, ecosystems & environment*, *136*(3-4), 292-300.

Gonçalves, D. R. P., de Moraes Sá, J. C., Mishra, U., Cerri, C. E. P., Ferreira, L. A., & Furlan, F. J. F. (2017). Soil type and texture impacts on soil organic carbon storage in a sub-tropical agro-ecosystem. *Geoderma*, 286, 88-97.

Guo Jing, Bo Wang, Guibin Wang, Sai Tay Zar Myo, Fuliang Cao. (2020). Effects of three cropland afforestation practices on the vertical distribution of soil organic carbon pools and nutrients in eastern China. *Global Ecology and Conservation*, 22, e00913.

He, W., Dutta, B., Grant, B. B., Chantigny, M. H., Hunt, D., Bittman, S., Tenuta, M., Worth, D., VanderZaag, A., Desjardins, R.L. and Smith, W.N. (2020). Assessing the effects of manure application rate and timing on nitrous oxide emissions from managed grasslands under contrasting climate in Canada. *Science of The Total Environment*, *716*, 135374.

Henry, M., Tittonell, P., Manlay, R. J., Bernoux, M., Albrecht, A., & Vanlauwe, B. (2009). Biodiversity, carbon stocks and sequestration potential in aboveground biomass in smallholder farming systems of western Kenya. *Agric Ecosyst Environ*, *129*(1-3), 238-252.

Hickman, J. E., Palm, C. A., Mutuo, P., Melillo, J. M., & Tang, J. (2014). Nitrous oxide (N2O) emissions in response to increasing fertilizer addition in maize (Zea mays L.) agriculture in western Kenya. Nutrient Cycling in Agroecosystems, 100(2), 177-187.

Hickman, J. E., Tully, K. L., Groffman, P. M., Diru, W., & Palm, C. A. (2015). A potential tipping point in tropical agriculture: Avoiding rapid increases in nitrous oxide fluxes from agricultural intensification in Kenya. Journal of Geophysical Research: Biogeosciences, 120(5), 938-951.

Huang, L., Liu, J., Shao, Q., & Xu, X. (2012). Carbon sequestration by forestation across China: Past, present, and future. *Renewable and Sustainable Energy Reviews*, 16(2), 1291-1299.

Ishizuka, S., Mori, T., Nakayama, Y., Kawabata, C., Konda, R., Sasaki, T., ... & Ohta, S. (2021). Effects of conversion from leguminous acacia to non-leguminous eucalyptus on soil N2O emissions in tropical monoculture plantations. *Ecol. Manag.*, *481*, 118702.

Islam, K. R., & Weil, R. R. (2000). Land use effects on soil quality in a tropical forest ecosystem of Bangladesh. *Agriculture, Ecosystems & Environment*, *79*(1), 9-16.

Jaetzold ,R,.Schmidt,H.,Hornet,Z.B.,Shisanya,C.A.,2010. Farm Management Hand-book of Kenya. Natural Conditions and Farm Information vol. 11/ Nyanza province, Siaya county, 2nd edition.Ministry of Agriculture/GTZ, Nairobi Kenya.

Jarecki, M., Grant, B., Smith, W., Deen, B., Drury, C., VanderZaag, A., Qian, B., Yang, J. and Wagner-Riddle, C (2018). Long-term trends in corn yields and soil carbon under diversified crop rotations. *Journal of environmental quality*, *47*(4), 635-643.

Jiang, R., Yang, J. Y., Drury, C. F., He, W., Smith, W (2021). Assessing the impacts of diversified crop rotation systems on yields and nitrous oxide emissions in Canada using the DNDC model. *Science of the Total Environment*, *759*, 143433

Kadiri, W. O. J., Fasina, A. S., & Babalola, T. S. (2021). Soil organic carbon concentration and stock of arable land use of two agro-ecological zones of Nigeria. *Journal of the Saudi Society of Agricultural Sciences*, 20(3), 180-189.

Kanyenji, G. M., Oluoch-Kosura, W., Onyango, C. M., & Karanja Ng'ang'a, S. (2020). Prospects and constraints in smallholder farmers' adoption of multiple soil carbon enhancing practices in Western Kenya. *Heliyon*, 6(3), e03226.

Kennedy-Perkins, R. S. (2022). *Methanogenesis, our greatest nemesis: How can farmers reduce greenhouse gases on-farm?* (Doctoral dissertation, University of Otago).

Kiboi M. N., Felix K. Ngetich, Anne Muriuki, Noah Adamtey, Daniel Mugendi. (2020). The response of soil physicochemical properties to tillage and soil fertility resources in Central Highlands of Kenya. *Italian Journal of Agronomy*15:1381.

Kiboi, M. N., Ngetich, K. F., Fliessbach, A., Muriuki, A., & Mugendi, D. N. (2019). Soil fertility inputs and tillage influence on maize crop performance and soil water content in the Central Highlands of Kenya. Agricultural Water Management, 217, 316-331.

Kihara J, Bolo P, Kinyua M, Nyawira SS, Sommer R (2020) Soil health and ecosystem services: lessons from sub-Sahara Africa (SSA). *Geoderma* 370:114342.

Kim, D. G., Kirschbaum, M. U., & Beedy, T. L. (2016). Carbon sequestration and net emissions of CH4 and N2O under agroforestry: Synthesizing available data and suggestions for future studies. Agriculture, Ecosystems & Environment, 226, 65-78.

Kumi, J. A., Kyereh, B., Ansong, M., & Asante, W. (2021). Influence of management practices on stand biomass, carbon stocks and soil nutrient variability of teak plantations in a dry semi-deciduous forest in Ghana. Trees, Forests and People, 3, 100049.

Li C (2012) User's guide for the DNDC model (version 9.5). Institute for the Study of earth, oceans and space, University ofnew Hampshire, Durham, NC, USA

Li C, Frolking S, Frolking TA (1992) A model of nitrous oxide evolution from soil driven by rainfall events: 1. Model struc- ture and sensitivity. *J Geophys Res Atmos* 97:9759–9776

Li, C. S. (2000). Modeling trace gas emissions from agricultural ecosystems. In *Methane emissions from major rice ecosystems in Asia* (pp. 259-276). *Springer, Dordrecht*.

Li, C., Frolking, S., & Harriss, R. (1994). Modeling carbon biogeochemistry in agricultural soils. *Global biogeochemical cycles*, *8*(3), 237-254.

Li, H., Qiu, J., Wang, L., Tang, H., Li, C., & Van Ranst, E. (2010). Modelling impacts of alternative farming management practices on greenhouse gas emissions from a winter wheat–maize rotation system in China. *Agriculture, ecosystems & environment*, *135*(1-2), 24-33.

Li, Z., Yang, J. Y., Drury, C. F., Yang, X. M., Reynolds, W. D., Li, X., & Hu, C. (2017). Evaluation of the DNDC model for simulating soil temperature, moisture and respiration from monoculture and rotational corn, soybean and winter wheat in

Canada. *Ecological Modelling*, *360*, 230-243.

Liang, L. L., Grantz, D. A., & Jenerette, G. D. (2016). Multivariate regulation of soil CO2 and N2O pulse emissions from agricultural soils. Global Change Biology, 22(3), 1286-1298.

Liao, J. D., & Boutton, T. W. (2008). Soil microbial biomass response to woody plant invasion of grassland. *Soil Biology and Biochemistry*, 40(5), 1207-1216.

Lu, M., Zhou, X., Luo, Y., Yang, Y., Fang, C., Chen, J., & Li, B. (2011). Minor stimulation of soil carbon storage by nitrogen addition: a meta-analysis. *Agriculture, ecosystems & environment*, 140(1-2), 234-244.

Luo, Z., Wang, E., & Sun, O. J. (2010). Soil carbon change and its responses to agricultural practices in Australian agroecosystems: a review and synthesis. *Geoderma*, 155(3-4), 211-223.

Lyon, C., Saupe, E. E., Smith, C. J., Hill, D. J., Beckerman, A. P., Stringer, L.C., Marchant, R., McKay, J., Burke, A., O'Higgins, P.& Aze, T. (2022). Climate change research and action must look beyond 2100. *Global Change Biology*, *28*(2), 349-361.

Macharia JM, Pelster DE, Ngetich FK, Shisanya CA, Mucheru- Muna M, Mugendi DN (2020) Soil greenhouse gas fluxes from maize production under different soil fertility manage- ment practices in East Africa. *J Geophys Res Biogeosci* 125: e2019JG005427

Macharia, J. M., Ngetich, F. K., & Shisanya, C. A. (2021). Parameterization, calibration and validation of the DNDC model for carbon dioxide, nitrous oxide and maize crop performance estimation in East Africa. *Heliyon*, *7*(5), e06977.

Macharia, J. M., Pelster, D. E., Ngetich, F. K., Shisanya, C. A., Mucheru-Muna, M., & Mugendi, D. N. (2020). Soil greenhouse gas fluxes from maize production under different soil fertility management practices in East Africa. *Journal of Geophysical Research: Biogeosciences*, *125*(7), e2019JG005427.

Martín, J. R., Álvaro-Fuentes, J., Gonzalo, J., Gil, C., Ramos-Miras, J. J., Corbí, J. G., & Boluda, R. (2016). Assessment of the soil organic carbon stock in Spain. *Geoderma*, 264, 117-125.

McNaughton, S. J., Banyikwa, F. F., & McNaughton, M. M. (1997). Promotion of the cycling of diet-enhancing nutrients by African grazers. *Science*, 278(5344), 1798-1800.

Midega, C. A., Wasonga, C. J., Hooper, A. M., Pickett, J. A., & Khan, Z. R. (2017). Drought-tolerant Desmodium species effectively suppress parasitic striga weed and improve cereal grain yields in western Kenya. Crop Protection, 98, 94-101.

Mishra Gaurav, Avishek Sarkar. (2020). Studying the relationship between total organic carbon and soil carbon pools under different land management systems of Garo hills, Meghalaya. *Journal of Environmental Management* 257, 110002.

Morisada, K., Ono, K., & Kanomata, H. (2004). Organic carbon stock in forest soils in Japan. *Geoderma*, 119(1-2), 21-32.

Muhati, G. L., Olago, D., & Olaka, L. (2018). Quantification of carbon stocks in Mount Marsabit Forest Reserve, a sub-humid montane forest in northern Kenya under anthropogenic disturbance. Global Ecology and Conservation, 14, e00383.

Musafiri CM, Macharia JM, Kiboi MN, Ng’etich OK, Shisanya CA, Okeyo JM, Mugendi DN, Okwuosa EA, Ngetich FK (2020a) Soil greenhouse gas fluxes from maize cropping system under different soil fertility management technologies in Kenya. *Agric Ecosyst Environ* 301:107064.

Musafiri, C. M., Macharia, J. M., Kiboi, M. N., Ng’etich, O. K., Shisanya, C.A., Okeyo, J.M., Okwuosa, E.A. and Ngetich, F.K. (2021). Comparison between observed and DeNitrification-DeComposition model-based nitrous oxide fluxes and maize yields under selected soil fertility management technologies in Kenya. *Plant and Soil*, *463*(1), 395-413.

Musafiri, C.M., Macharia, J.M., Ng'etich, O.K., Kiboi, M.N., Okeyo, J., Shisanya, C.A., Okwuosa, E.A., Mugendi, D.N., Ngetich, F.K., (2020b). Farming systems’ typologies analysis to inform agricultural greenhouse gas emissions potential from smallholder rain-fed farms in Kenya. *Sci. Afr* , 8, e00458.

Mutegi, J. K., Munkholm, L. J., Petersen, B. M., Hansen, E. M., & Petersen, S. O. (2010). Nitrous oxide emissions and controls as influenced by tillage and crop residue management strategy. Soil Biology and Biochemistry, 42(10), 1701-1711.

Muui, C.W., Muasya, R.M., Kirubi, D.T., 2013. Baseline survey on factors affecting sorghum production and use in eastern Kenya. *J. Food, Agric. Nutr*. 13, 7339-7353.

Namirembe, S., Piikki, K., Sommer, R., Söderström, M., Tessema, B., & Nyawira, S. S. (2020). Soil organic carbon in agricultural systems of six countries in East Africa–a literature review of status and carbon sequestration potential. South African Journal of Plant and Soil, 37(1), 35-49.

Ndung'u, M., Ngatia, L. W., Onwonga, R. N., Mucheru-Muna, M. W., Fu, R., Moriasi, D. N., & Ngetich, K. F. (2021). The influence of organic and inorganic nutrient inputs on soil organic carbon functional groups content and maize yields. *Heliyon*, 7(8), e07881.

Negash, M., & Starr, M. (2015). Biomass and soil carbon stocks of indigenous agroforestry systems on the south-eastern Rift Valley escarpment, Ethiopia. *Plant and soil*, 393(1), 95-107.

Ngetich, K. F., Diels, J., Shisanya, C. A., Mugwe, J. N., Mucheru-Muna, M., & Mugendi, D. N. (2014). Effects of selected soil and water conservation techniques on runoff, sediment yield and maize productivity under sub-humid and semi-arid conditions in

Kenya. Catena, 121, 288-296.

Ngome, A. F., Becker, M., Mtei, M. K., & Mussgnug, F. (2013). Maize productivity and nutrient use efficiency in Western Kenya as affected by soil type and crop management. *International Journal of Plant Production*, *7*(3), 517-536.

Njagi, T., Onyango, K., Kirimi, L., & Makau, J. (2019). *Sorghum Production in Kenya: Farm-level Characteristics, Constraints and Opportunities*. Tegemeo Institute.

Nyawira, S. S., Hartman, M. D., Nguyen, T. H., Margenot, A. J., Kihara, J., Paul, B.K., Williams, S., Bolo, P. and Sommer, R. (2021). Simulating soil organic carbon in maize-based systems under improved agronomic management in Western Kenya. *Soil and Tillage Research,* 211, 105000.

Obi-Njoku, O. (2022). Estimating greenhouse gas emissions from land-applied biosolids in Canada: A mathematical modelling approach.

Oertel, C., Matschullat, J., Zurba, K., Zimmermann, F., & Erasmi, S. (2016). Greenhouse gas emissions from soils—A review. Geochemistry, 76(3), 327-352.

Okalebo JR, Gathua KW, Woomer PL. (2002). Laboratory methods of soil and plant analysis: a working manual second edition. Nairobi: TSBFCIAT and SACRED Africa.

Ondier, J., Okach, D.O., John, O.C., Otieno, D.O., 2020. Influence of rainfall amount and livestock grazing on soil respiration in a moist Kenyan savannah. *Afr. J. Ecol*. 58, 92-99.

Ortiz-Gonzalo, D., de Neergaard, A., Vaast, P., Suárez-Villanueva, V., Oelofse, M., & Rosenstock, T. S. (2018). Multi-scale measurements show limited soil greenhouse gas emissions in Kenyan smallholder coffee-dairy systems. Science of the Total Environment, 626, 328-339.

Ortiz-Gonzalo, D., Vaast, P., Oelofse, M., de Neergaard, A., Albrecht, A., & Rosenstock, T. S. (2017). Farm-scale greenhouse gas balances, hotspots and uncertainties in smallholder crop-livestock systems in Central Kenya. Agriculture, Ecosystems & Environment, 248, 58-70.

Pachauri, R. K., & Meyer, L. A. (2014). Climate Change 2014: Synthesis Report. Contribution of Working Groups I, II and III to the Fifth Assessment Report of the Intergovernmental Panel on Climate Change.

Pardo, M. T., Almendros, G., Zancada, M. C., & Lopez-Fando, C. (2010). Biofertilization of degraded Southern African soils with cyanobacteria affects organic matter content and quality. *Arid Land Research and Management*, *24*(4), 328-343.

Parkin, T. B., & Venterea, R. T. (2010). USDA-ARS GRACEnet Project Protocols Chapter 3. Chamber-Based Trace Gas Flux Measurements 4.

Parkin, T. B., Venterea, R. T., & Hargreaves, S. K. (2012). Calculating the detection limits of chamber-based soil greenhouse gas flux measurements. Journal of environmental quality, 41(3), 705-715.

Parry, R. Soil-Plant-Atmosphere-Water Field & Pond Hydrology.

Pelster, D., Rufino, M., Rosenstock, T., Mango, J., Saiz, G., Diaz-Pines, E., Baldi, G. and Butterbach-Bahl, K., (2017). Smallholder farms in eastern African tropical highlands have low soil greenhouse gas fluxes. *Biogeosciences*. 14, 187-202.

Pelster, D.E., Gisore, B., Goopy, J., Korir, D., Koske, J.K., Rufino, M.C., Butterbach-Bahl, K., (2016). Methane and nitrous oxide emissions from cattle excreta on an East African grassland. *J. Environ. Qual*.45, 1531-1539.

Polasky, S., Nelson, E., Pennington, D., & Johnson, K. A. (2011). The impact of land-use change on ecosystem services, biodiversity and returns to landowners: a case study in the state of Minnesota. *Environmental and Resource Economics*, *48*(2), 219-242.

Qiu, L., Wei, X., Zhang, X., & Cheng, J. (2013). Ecosystem carbon and nitrogen accumulation after grazing exclusion in semiarid grassland. *PloS one*, 8(1), e55433

Radeny, M., Mungai, C., Amwata, D., Osumba, J., & Solomon, D. (2020). Climate change, agriculture, food and nutrition security policies and frameworks in Kenya. *CCAFS Working Paper*.

Rafique R, Peichl M, Hennessy D, Kiely G (2011) Evaluating management effects on nitrous oxide emissions from grass- lands using the process-based DeNitrification–DeComposition (DNDC) model. *Atmos Environ* 45:6029– 6039

Rahman, N., Giller, K. E., de Neergaard, A., Magid, J., van de Ven, G., & Bruun, T. B. (2021). The effects of management practices on soil organic carbon stocks of oil palm plantations in Sumatra, Indonesia. Journal of Environmental Management, 278, 111446.

Ren, B., Chen, P., Shaaban, M., Yang, X., Chen, Y., Zhang, Z., ... & Núñez-Delgado, A. (2022). Appraisal of different land use systems for heterotrophic respiration in a Karst landscape. *Environmental Research*, 113480.

Reppin, S., Kuyah, S., de Neergaard, A., Oelofse, M., & Rosenstock, T. S. (2020). Contribution of agroforestry to climate change mitigation and livelihoods in Western Kenya. *Agroforestry Systems*, *94*(1), 203-220.

Reszkowska, A., Krümmelbein, J., Peth, S., Horn, R., Zhao, Y., & Gan, L. (2011). Influence of grazing on hydraulic and mechanical properties of semiarid steppe soils under different vegetation type in Inner Mongolia, China. *Plant and Soil*, 340(1), 59-72.

Rosenstock, T.S., Mpanda, M., Pelster, D.E., Butterbach-Bahl, K., Rufino, M.C., Thiong'o, M., Mutuo, P., Abwanda, S., Rioux, J., Kimaro, A.A. and Neufeldt, H., (2016).

Greenhouse gas fluxes from agricultural soils of Kenya and Tanzania. *J. Geophys. Res*. 121, 1568-1580.

Ryan, J., Estefan, G., & Rashid, A. (2001). *Soil and plant analysis laboratory manual*. ICARDA.

Saidy, A. R., Smernik, R. J., Baldock, J. A., Kaiser, K., & Sanderman, J. (2013). The sorption of organic carbon onto differing clay minerals in the presence and absence of hydrous iron oxide. *Geoderma*, 209, 15-21.

Sarto, M. V., Borges, W. L., Sarto, J. R., Rice, C. W., & Rosolem, C. A. (2020). Deep soil carbon stock, origin, and root interaction in a tropical integrated crop–livestock system. *Agroforestry Systems*, 94, 1865-1877.

Sarvade, S., Singh, R., Prasad, H., & Prasad, D. (2014). Agroforestry practices for improving soil nutrient status. *Popular Kheti*, *2*(1), 60-64.

Schmidt, M. W., Torn, M. S., Abiven, S., Dittmar, T., Guggenberger, G., Janssens, I. A., ... & Trumbore, S. E. (2011). Persistence of soil organic matter as an ecosystem property. *Nature*, *478*(7367), 49-56.

Serrano-Silva, N., Sarria-Guzmán, Y., Dendooven, L., Luna-Guido, M., (2014). Methanogenesis and methanotrophy in soil: a review. *Pedosphere*, 24, 291-307.

Shan, J., Yan, X. (2013). Effects of crop residue returning on nitrous oxide emissions in agricultural soils. *Atmos. Environ*. 71, 170-175.

Silveira, M. L., Xu, S., Adewopo, J., Franzluebbers, A. J., & Buonadio, G. (2014). Grazing land intensification effects on soil C dynamics in aggregate size fractions of a Spodosol. *Geoderma*, 230, 185-193.

Six, J., Conant, R. T., Paul, E. A., & Paustian, K. (2002). Stabilization mechanisms of soil organic matter: implications for C-saturation of soils. *Plant and soil*, 241(2), 155-176.

Smith, P. (2008b). Land use change and soil organic carbon dynamics. *Nutrient Cycling in Agroecosystems*, *81*(2), 169-178.

Smith, P., (2016). Soil carbon sequestration and biochar as negative emission technologies. *Glob. Chang. Biol*. 22, 1315–1324.

Smith, P., Martino, D., Cai, Z., Gwary, D., Janzen, H., Kumar, P., McCarl, B., Ogle, S., O'Mara, F., Rice, C. & Smith, J. (2008). Greenhouse gas mitigation in agriculture. Philosophical transactions of the royal Society B: Biological Sciences, 363(1492), 789-813.

Smith, W. N., Grant, B. B., Desjardins, R. L., Rochette, P., Drury, C. F., & Li, C. (2008). Evaluation of two process-based models to estimate soil N2O emissions in Eastern Canada. *Canadian Journal of Soil Science*, *88*(2), 251-260.

Sommer R, Paul BK, Mukalama J, Kihara J. (2018). Reducing losses but failing to sequester carbon in soils – the case of Conservation Agriculture and Integrated Soil Fertility Management in the humid tropical agroecosystem of western Kenya. *Agriculture, Ecosystems and Environment* 254: 82–91.

Song, B. L., Yan, M. J., Hou, H., Guan, J. H., Shi, W. Y., Li, G. Q., & Du, S. (2016). Distribution of soil carbon and nitrogen in two typical forests in the semiarid region of the Loess Plateau, China. *Catena*, *143*, 159-166.

Stavi, I., Ungar, E. D., Lavee, H., & Sarah, P. (2008). Grazing-induced spatial variability of soil bulk density and content of moisture, organic carbon and calcium carbonate in a semi-arid rangeland. *Catena*, 75(3), 288-296.

Swanepoel, C. M., Van der Laan, M., Weepener, H. L., Du Preez, C. C., & Annandale, J. G. (2016). Review and meta-analysis of organic matter in cultivated soils in southern Africa. *Nutrient cycling in agroecosystems*, 104(2), 107-123.

Tanveera, A., Kanth, T. A., Tali, P. A., & Naikoo, M. (2016). Relation of soil bulk density with texture, total organic matter content and porosity in the soils of Kandi Area of Kashmir valley, India. *Int. Res. J. Earth Sci*, *4*(1), 1-6.

Tian, H., Melillo, J., Lu, C., Kicklighter, D., Liu, M., Ren, W., ... & Running, S. (2011). China's terrestrial carbon balance: contributions from multiple global change factors. *Global Biogeochemical Cycles*, 25(1).

Tongwane, M., Mdlambuzi, T., Moeletsi, M., Tsubo, M., Mliswa, V., Grootboom, L., (2016). Greenhouse gas emissions from different crop production and management practices in South Africa *Environ. Dev* , 19, 23-35.

Tubiello, F. N. (2019). Greenhouse gas emissions due to agriculture.

Tubiello, F.N., Salvatore, M., Rossi, S., Ferrara, A., Fitton, N., Smith, P., (2013). The FAOSTAT database of greenhouse gas emissions from agriculture. *Environ. Res. Lett*.8, 015009.

Uzoma KC, Smith W, Grant B, Desjardins RL, Gao X, Hanis K, Tenuta M, Goglio P, Li C (2015) Assessing the effects of agricultural management on nitrous oxide emissions using flux measurements and the DNDC model. *Agric Ecosyst Environ* 206:71–83.

Valentini, R., Arneth, A., Bombelli, A., Castaldi, S., Cazzolla Gatti, R., Chevallier, F., Ciais, P., Grieco, E., Hartmann, J., Henry, M. and Houghton, R.A., (2014). A full greenhouse gases budget of Africa: synthesis, uncertainties, and vulnerabilities. *Biogeosciences*, *11*(2), 381-407.

Vanlauwe, B., AbdelGadir, A. H., Adewopo, J., Adjei-Nsiah, S., Ampadu-Boakye, T., Asare, R. & Dianda, M. (2017). Looking back and moving forward: 50 years of soil and soil fertility management research in sub-Saharan Africa. *International Journal of Agricultural Sustainability*, 15, 613-631.

Vanlauwe,B.,Six,J.,Sanginga, N ,.,& Adesina,A,A.(2015).Soil fertility decline at the base of rural poverty in sub-Sahara Africa, *Nature plants*,1(7),15101.

Vesterdal, L., Ritter, E., & Gundersen, P. (2002). Change in soil organic carbon following afforestation of former arable land. *Forest ecology and management*, *169*(1-2), 137-147.

Wachiye Sheila, Lutz Merbold, Timo Vesala, Janne Rinne, Matti Räsänen, Sonja Leitner, & Petri Pellikka. (2020). Soil greenhouse gas emissions under different land-use systems in savanna ecosystems of Kenya. *Biogeosciences*, 17, 2149–2167.

Wachiye, S., Merbold, L., Vesala, T., Rinne, J., Leitner, S., Räsänen, M., Vuorinne, I., Heiskanen, J., Pellikka, P., (2021). Soil greenhouse gas emissions from a sisal chronosequence in Kenya. *Agric For Meteorol*. 307, 108465.

Wanyama, I., Pelster, D. E., Butterbach-Bahl, K., Verchot, L. V., Martius, C., & Rufino, M. C., (2019). Soil carbon dioxide and methane fluxes from forests and other land use types in an African tropical montane region. *Biogeochemistry*. 143, 171-190.

Wanyama, I., Pelster, D.E., Arias-Navarro, C., Butterbach-Bahl, K., Verchot, L.V., Rufino, M.C., (2018a). Management intensity controls soil $N_2O$ fluxes in an Afromontane ecosystem. *Sci. Total Environ*. 624, 769-780.

Wanyama, I., Rufino, M. C., Pelster, D. E., Wanyama, G., Atzberger, C., Van Asten, P., Verchot, L.V. and Butterbach-Bahl, K., (2018b). Land use, land use history, and soil type affect soil greenhouse gas fluxes from agricultural landscapes of the East African Highlands. *J. Geophys. Res. Biogeosci. J:* 123, 976-990.

Wei, L., Hai-Zhou, H., Zhi-Nan, Z., & Gao-Lin, W. (2011). Effects of grazing on the soil properties and C and N storage in relation to biomass allocation in an alpine meadow. *Journal of soil science and plant nutrition*, 11(4), 27-39.

Williams, D. R., Phalan, B., Feniuk, C., Green, R. E., & Balmford, A. (2018). Carbon storage and land-use strategies in agricultural landscapes across three continents. *Current Biology*, *28*(15), 2500-2505.

Xiang, N., Hassenrück, C., Pogoreutz, C., Rädecker, N., Simancas-Giraldo, S. M., Voolstra, C.R., Wild, C. & Gärdes, A. (2022). Contrasting microbiome dynamics of putative denitrifying bacteria in two octocoral species exposed to dissolved organic carbon (DOC) and warming. Applied and environmental microbiology, 88(2), e01886-21.

Zuo, X., Zhao, H., Zhao, X., Zhang, T., Guo, Y., Wang, S., & Drake, S. (2008). Spatial pattern and heterogeneity of soil properties in sand dunes under grazing and restoration in Horqin Sandy Land, Northern China. *Soil and Tillage Research*, 99(2), 202-212.